DI Dr. Johann Marton

DIPLOMARBEIT

Development and testing of an active shielding for SIDDHARTA–2

ausgeführt am

Atominstitut der Technischen Universität Wien

unter der Anleitung von DI Dr. Johann Marton

durch

Florian Schilling, BSc

Neubaugürtel 50/10, A-1070 Wien

Datum

Unterschrift (Student)

Development and testing of an active shielding for SIDDHARTA–2

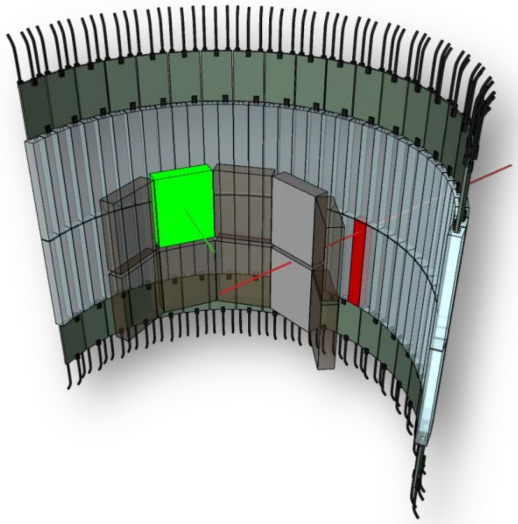

ABSTRACT

The SIDDHARTA experiment investigatedthe low-energy strong interaction with strangeness, employing kaonic hydrogen and kaonic deuterium. The experimental observables are the 1s state shift and width of these atoms.The acronym SIDDHARTA stands for Silicon Drift Detector for Hadronic Atom Research by Timing Application.

The experiment on kaonic hydrogen was successfully performed in 2009. However, the kaonic deuterium measurement suffered from low signal strength and a high background signal. To take a step further SIDDHARTA-2 should correct these insufficiencies with better shielding and other improvements. The experiment will beconducted in 2013/2014.

The goal of this diploma thesis is to providea solution forthe reduction of the hadronic background with an active shielding mechanism. This will be located around the SDDx-ray detector ring and should be accomplished in a preferable simple and low cost apparatus. This ring-shaped detector arrangementwill consist of scintillation counters providing the largest detection area possible and is read-out by solid state photo detectors (SiPMs, See *2.2*).

The SIDDHARTA setup is mounted inside a vacuum chamber, therefore the shielding has to work in such an environment. Furthermore at least hundred SiPMs have to be powered and read out, so a small preamplifier with power source has to bedeveloped. In this diploma thesis, different power source types are tested, as well as various scintillator shapes and SiPM characteristics.

TABLE OF CONTENTS

1 INTRODUCTION

This chapter provides a general overview over the physics and the **SIDDHARTA** experiment (What is SIDDHARTA? See 1.1). [1-3]The current studies are dealing with the tests and developmentof an active shielding (veto-system) which should improve the signal-to-noise-ratio. In SIDDHARTA-2 [4, 5] it will veto unwanted events (pions, cosmic radiation etc.) and is planned to consist of a ring of scintillators around the Silicon Drift Detector (SDD) measuring system. The activeshielding's measuring unit will provide the veto data for the electronics. The conclusion of this work will help to design and study the possibilities of this SIDDHARTA-2 setup improvement.

This part gives a very simple explanation of the physics behind the SIDDHARTA-2 experiment.

Hadrons are particles that are influenced by the nuclear force(strong interactions that hold together the nucleus of an atom). The nuclear force has a very short range and is stronger than the electrical force in the nuclear regime (which would repel two protons). Hadronic representatives are the proton and the neutron, (both so called baryons)which can be found in the atoms of our periodic system.

Hadrons consist of **quarks**, the fundamental particles of matter. They are combined to form subatomic particles like the neutron or the proton. Six types, also known as flavours, exist: up, down, charm, strange, bottom, top and their antimatter equivalents (anti-up,…). Up and down quarks are the lightest of their kind, they build protons (up, up, down) and neutrons (up, down, down).

Quarks can not only form baryons (proton/neutron) but also **mesons**.These unstable particles consistof a quark and antiquark. Due to their hadronic inheritance, they are also affected by strong interactions. This is the reason for using them in SIDDHARTA for strong interaction research.

Kaons come in various kinds: K^+, K^-, K^0 with K^- as the most importantparticle for the SIDDHARTA experiment, since only this can form a kaonic exotic atom. The K^-consists of strange and anti-up quarks and is combiningwith a proton to kaonichydrogen/deuterium.(K^-has a negative charge.)In kaonic atoms the kaon acts electromagnetically like a heavy electron but also shows strong interaction with the nucleus.

Excited atoms try to minimize their energy with releasing energy in **transitions** between quantum levels. In lower states x-ray transitions are preferred, thus photons with an energy equivalent to the energy loss can be detected. In equilibrium (the ground state) the electron of a hydrogen atom is located on the 1s level. (See fig. 1.1)

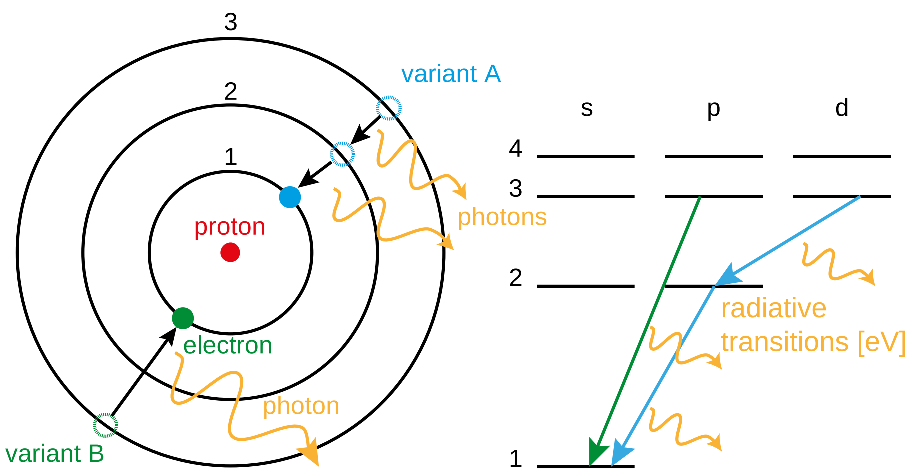

fig.1.1 Simple scheme of transitions in the radiative hydrogen atom.
Variant Kα and Kβ are only two of many possibilities of x-ray transitions. The transition energy is usually in the order of eV. This energy can be measured with a detector.

1.1 What is SIDDHARTA?

The SIDDHARTA experiment is aiming at the investigation of the low-energy strong interaction involving strangeness using kaonic hydrogen and kaonic deuterium as probes. The acronym SIDDHARTA stands for **Si**liconD**r**ift **D**etector for **H**adronic **A**tom **R**esearch by **T**iming **A**pplication. The experiment was finished in 2009 (at DAΦNE collider, Frascati, Italy) and determined the shift and width of the kaonic hydrogen atom. (See following fig. 1.2)

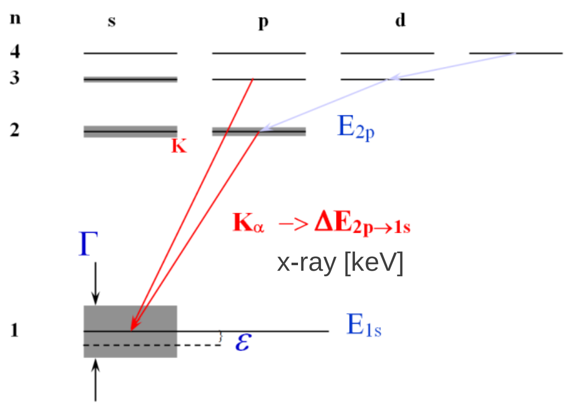

fig.1.2 Shift and width of kaonic hydrogen atoms
Substituting the electron with a kaon (K^-) results in a shift ε (the position of 1s is different compared to natural atoms) and a width of Γ (the energy of the ground level is broadened in kaonic atoms). The transition energy as a consequenceof the high reduced mass is in the order of several keV (which is 1000 times the energy of the hydrogen atom transitions).

The modification of the 1s state (width and shift) due to strong interactions is correlated to kaon-proton and kaon-neutron scattering lengths, which are related to isospin dependent scattering lengths. The extraction of this scattering length from the measurements of shift and width is rather complicated and is investigated in theoretical physics. With the isospin dependency of the scattering length, knowledge about low energy QCD [5, 6] in the strangeness sector can be obtained. The investigations will give the strong interaction parameters at the threshold (real and imaginary part of the scattering length described by low energy QCD)and new information about the kaon sub-threshold resonance Λ(1405).

1.2 Improvements for SIDDHARTA-2

Within SIDDHARTA-2 studies on kaonic deuterium are foreseen. In order to perform the x-ray measurements, better shielding, calibrations and improvements of the geometry are mandatory. These modifications are optimized by Monte Carlo simulations.

SDDs [7,8] will be used and positioned closer to the target cell, thisprovides faster drift time as well as a better noise reduction. The target cell will be cooled to stop more kaons due to a higher gas density, which results in a higher signal. To lower the noise, the passive shielding is improved as well as the target cell geometry, less cell material results in less fluorescence, when particles stop in it. Infig. 1.3 a top and

fig. 1.4 a side view of the new SIDDHARTA-2 setup is shown. To provide a better calibration, a new x-ray calibration scheme is foreseen.A kaon monitor will be positioned as close as possible to the entrance window, to increase the K^-- trigger events and a K^+- detector on the opposite side to confirm the negative charge. Further an active shielding – a veto (anticoincidence) system – will be positioned around the target cell in order to reject events which pass the shielding as well as detect unwanted hadronic background. (See following figures)

In this thesis I deal with this last improvement, the Detectors and thedevelopment of the active shielding.

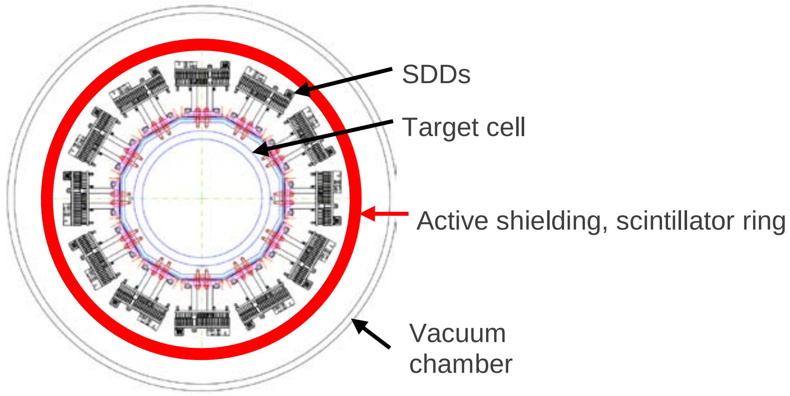

fig.1.3 SIDDHARTA-2 target cell design and SDD arrangement (top view). Red circle: the active shielding.

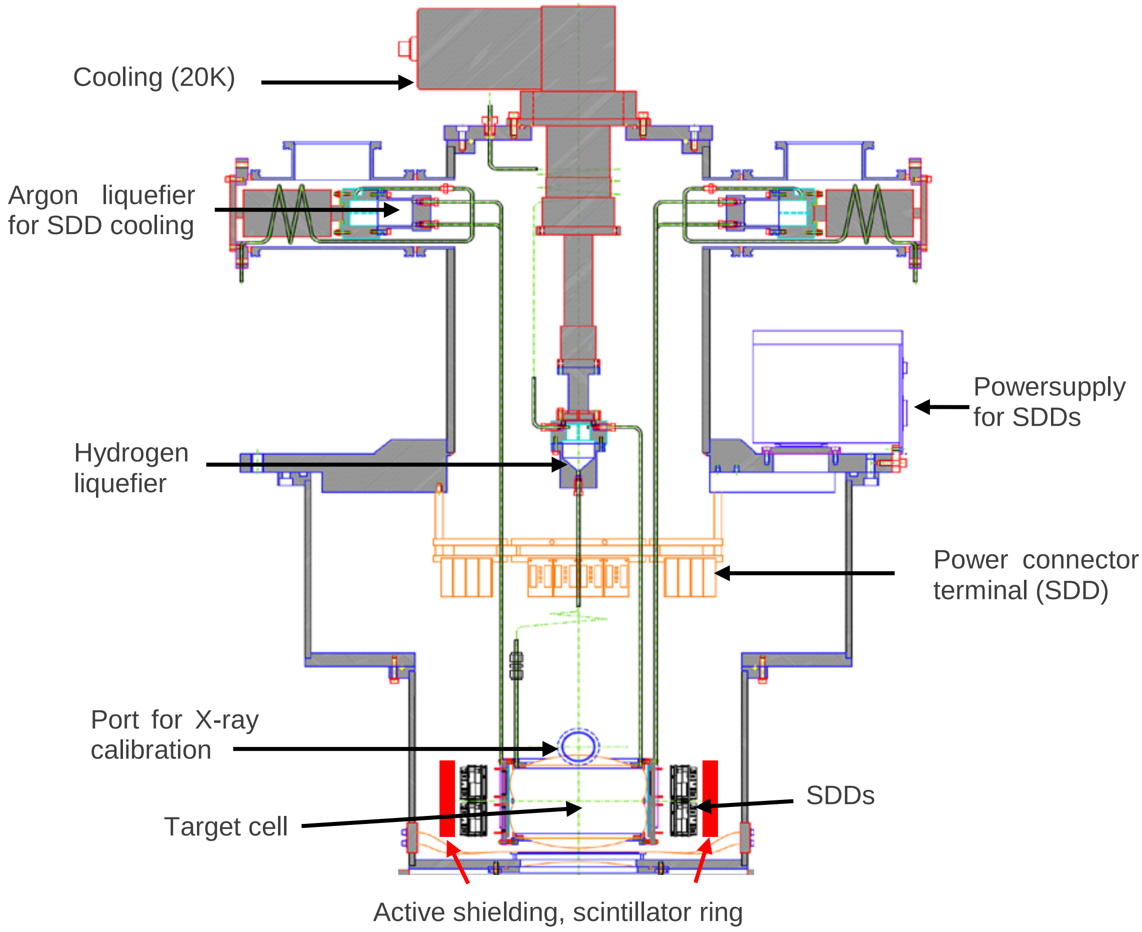

fig. 1.4 Side view of the SIDDHARTA-2 setup.

1.3 TASKS

My work prior to this thesis was to study the possibilities of detector units for the active shielding that will be located around the SDD x-ray detector array. To provide a good, reliable and low priced detector we want to use a system [9] containing a scintillator,a SiPM (Silicon Photo Multiplier, see *2.2, p. 11*)and a preamplifier. To achieve high flexibility at minimal space we considered to upgrade the preamplifier with a power supply for the SiPM (around 70V) and an on-board trigger. I characterized the preamplifier linearity and a current respectively a voltage source prototype, as well as tested an on-board trigger in 3.7 (p.40).

To get an idea of the ideal scintillator/SiPM combinationI studied several shapes, wrappings and sizes of the material in combination with different SiPM positions (on thefront face; both ends) in 3.6 (p. 26). Further investigations in this chapter studied the timing of the combination and therefore the possibility of a rudimentary localization of particle hits on the scintillator.In 3.8(p. 50) the temperature dependency of the electronic parts was investigated. With the aim of studying the ability tocharacterizeincoming particles I also logged the charge ADC spectra.

The goal of this thesis was to develop and test a dedicated SiPM front-end electronic and find the best size trade-off for the scintillator. The system should work under vacuum conditions and compensate temperature variations by itself.

2 Preparations and setup

2.1 Scintillators

The scintillator material Iused in this thesis is a **plastic scintillator with fluorescent molecules** (PVT). The material is similar to acrylic glass but, when hit by particles or light, it emits light of the blue spectrum. This effect is induced by the excitation of molecules or atoms in the scintillating material. An incidental particle as well as secondary electrons from absorbed photons can stimulate other photons on their way through the scintillator. Not every photon reaches the detectorbecause some are absorbed and/or not fully reflected at the materials edges.

The signal of the detector is influenced by recombination effects in the scintillator and consists of a steep rising edge and a shallow trailing edge. There is a fast (fluorescent) and a slow (phosphorescent) part, which are summed up. The behaviour is given in the following fig. 2.1.

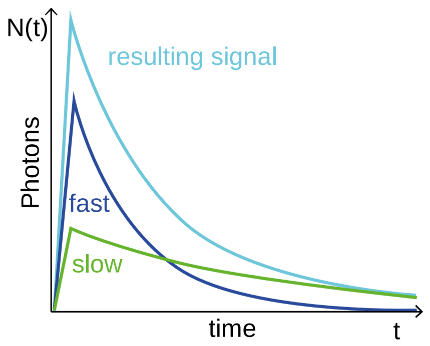

fig.2.1 Signal shape of a scintillator (schematic).
The diagram shows the influence of afast (fluorescent) and a slow (phosphorescent) part.

This theoretical shape is confirmed whenexamining the signal on the oscilloscope (see fig. 3.3,p.21).

Acrylic glass is very easy to handle and shape, but the sensitive material of plastic scintillators needsa more careful handling. To **maximize the photon yield** the surfaces have to be polishedand kept away from mechanical force, finger printsand high temperatures. These conditions have a negative effect and result in aging of the material, which can be seen as fine crazes on the surface. How I managed the polishing and handling can be read in2.1.1 (p. 8).

Five different scintillator dimensions were tested:

Size A: 10x15x200mm (or 210mm length)
Two SiPMs mounted at both ends/faces (two different scintillators, one with SiPM1 and SiPM2 mounted, the other withSiPM3 and SiPM4)

Size B: 10x20x73mm
One SiPM mounted on one front end of the scintillator.
(three scintillators: SiPM6, SiPM9 and SiPM10)

Size C: 10x10x20mm
An aluminium U-profile with one small scintillator at each end (SiPM1 and SiPM2) is used astrigger for coincidental measurements. See fig. 3.10(p. 28) respectively fig. 3.12 (top, p. 30)

Size D: 20x20x150mm
Four SiPMs (SiPM5, SiPM6, SiPM7 and SiPM8) mounted on one front end face as shown infig. 3.17 (p. 33).

Size E: 31x39x377mm
Two SiPMs (SiPM9 and SiPM10) mounted horizontally, approximately in the middle of onefront end face with the pins located at the centre.

For specification of the SiPMs see 5.2.2 in the appendix.

2.1.1 Polishing process

Polishing scintillators is a challenging process. I tested several methods, with varying degrees of success. Asmooth and transparent surfacecan be achieved by polishing thesurfaces with **sandpapers** of different grain sizes. Themost successful process took placeon a glass plate under flowing water. To preventbouncing of the scintillator block, only little pressure and small motionswere to be applied. (1cm movement straight or circled, at least four turnings of 90° to polish every edge and avoid bevel, see fig. 2.2 below)

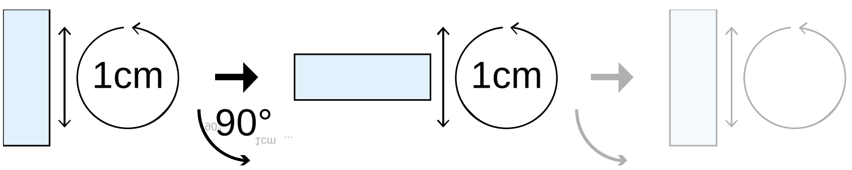

fig.2.2 Scintillator movement in the polishing process

To ensure that the surface is not contaminated with finger prints, I wear latex gloves (they also increase the grip and enhance the endurance in cold water).

While using finest polishing papers (grain size >8000) there is a possibility to cause **deep scratches** due to the friction heat (even in spite of great care).The best way to avoid this is to polish with the paper wrapped around a finger and frequently flushingit with water.

The last step is using **diamond polishing** paste to clear the surface of possible bloom and to remove smallest scratches. First I applied a small amount of the paste on a cloth and after the surface is well polished but bloomy, I used a dry piece of cloth to fine polish it with the residue of the paste. Since this whole step can chamfer the edges one has to becareful and to try to keep it short.

After polishing, the surface should be cleaned with **soap and water** to clear it from grease. The following fig. 2.3 shows pictures of the whole process.

Rough polishing on a glass plate under flowing water.

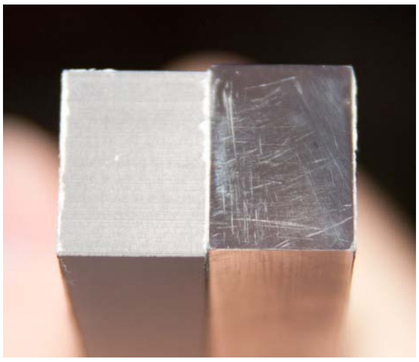

Left: raw material (milled).
Right: after rough polishing.

Freehand fine polishing withcontinuous flushing.

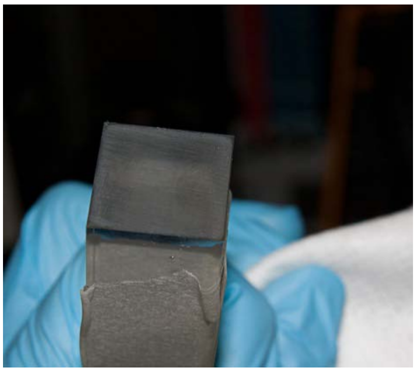

Visible blooming.

Diamond paste polishing to clear the scintillator of blooming.

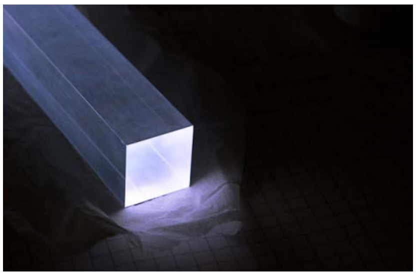

Scintillator after cleaning with soap and water.

fig.2.3 Pictures of the scintillator polishing process
The process takes place in several steps: Polishing with sand paper of several grain sizes, finalizing with diamond paste and cleaning with soap and water afterwards.

Unsuccessful methods:

I experimented with polishing in a small amount of alcohol instead of the water jet.It turned out to bleach the sandpaper (maybe even destroy it) and negative effects to the scintillator cannot be ruled out.Fine-grained powders also did not improve the process.

Short list of the polishing process: (The numbers are the grain size)

1. 600 for flatteningrough unevenness'(constant flushing, glass plate)
2. 1200/2000 for further smoothing (constant flushing, glass plate)
3. >8000 for polishing(under flowing water, wrapped around a finger)
4. diamond polishing paste (if unevenness can be spotted, one has to redo the process starting at least with 2000)
5. soap and water to clear the surface of oil/grease

2.1.2 Wrapping the scintillator and attaching the SiPM

There are certain philosophies in case of wrapping a scintillator. There is one of using aluminium or a similar reflective foil for achieving good reflection results and there is the other, counting on diffuse scattering with **Teflonwrapping**. The first tests were made with a relatively inflexible and thick aluminium foil, which resulted in a comparatively weak signal (see 3.3, p. 20). Therefore in the later experiments the first layer always consisted of Teflon.fig. 2.4 shows the wrapping and the SiPM attaching process.

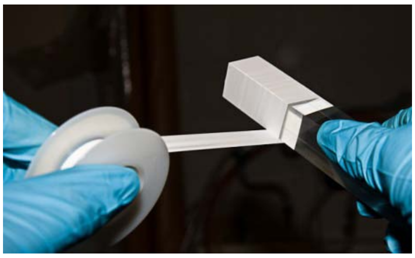

Wrapping with Teflon, tightly overlapping.

Adding two smooth and tight layers of aluminium foil.

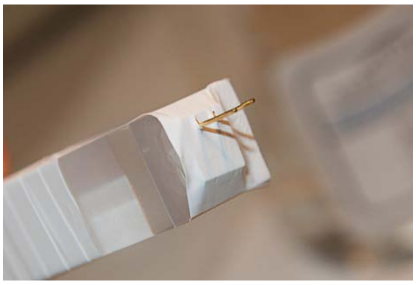

SiPM fixation with Teflon after application of optical grease (see appendix, 5.2.3)

Further SiPMfixation and tightening with isolating tape.

fig.2.4 Pictures of the scintillator wrapping and mounting
To achieve maximum light tightness, Teflon is wrapped around the scintillator first. After that, the surface is greased with a drop of optical grease and the SiPMs pins are thrustthroughthe Teflon band that I pulled down tightly. Depending on the experiment, aluminium foil is carefully wrapped around and everything is tightly surrounded with isolating tape (Where I cut slits for the diode pins inand appliedmore forcefor further fixation of the SiPM).

2.1.3 LIGHT TIGHTNESS TESTS

I checked the light tightness by reading out the charge ADC spectrum: First with the scintillator placed outside and afterwardsinside a box. fig. 2.5 shows that the spectra are nearly identical.The wrapping has at least one weak spot in case of light tightness. It is located at the contact point of the scintillator and the SiPM. The problem is that the SiPM needs a connection to the environment. I lead the pins through the isolating tape (trenchingtwo slits) and pinned them through the Teflon. My experiments showed that even with this lack of perfect light-sealing the impact is insignificant.

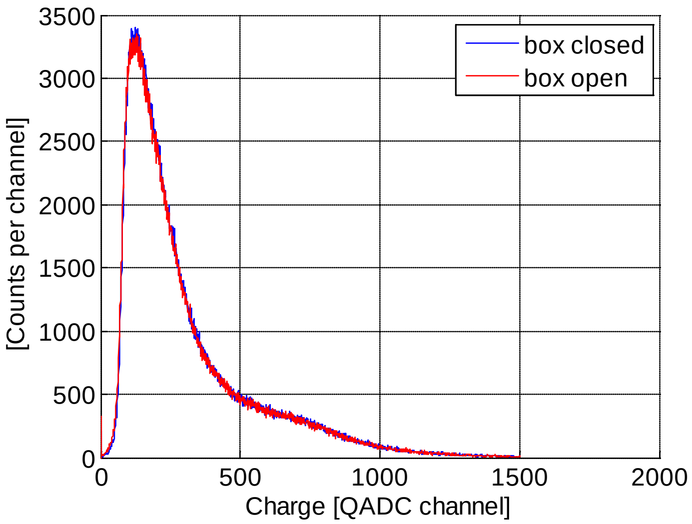

fig.2.5 Comparison of QADC spectra for light tightnessapprovement. (1 h acquiring)
To seal the setup from light, a carton box lined with black felt paper was put over. The spectrum of SiPM4 measuring the source (seeappendix, 5.2.10) located in the middle of the scintillator shows thatthe wrappingis light tight. (Same setup as in 3.2, p. 20)

2.2 SILICON PHOTO MULTIPLIER

SiPM is the short form of **Silicon Photo Multiplier** which in this thesis is synonymously used for PPD (Pixelized Photo Multiplier, one is shown in the followingfig. 2.6) [10,11]. In comparison to PMTs (Photo Multiplier Tube) or PMs (Photo Multiplier) the SiPM is a semiconductor and therefore much more compact than the tubes of the multipliers.

The photodiode uses the photoelectric effect to produce a signal from incoming photons. (The electrons of the material are releaseddue to the transferred photon energy and this initializes a breakthrough) To start the **avalanche effect** a high bias voltage (our examplesrequire around 70V)is necessary to set up a strong transition area, so even slow photons can initialize it. When initialized the freed electrons entrain others and this exponential breakthrough is called avalanche. The result is a firstbuilt-in amplification stage.

The SiPMs used in this thesis consist of a matrix of APDs.[1][12] mounted and sealed in a small ceramic case which isbiased and read out via 2 pins. (See following fig. 2.6)

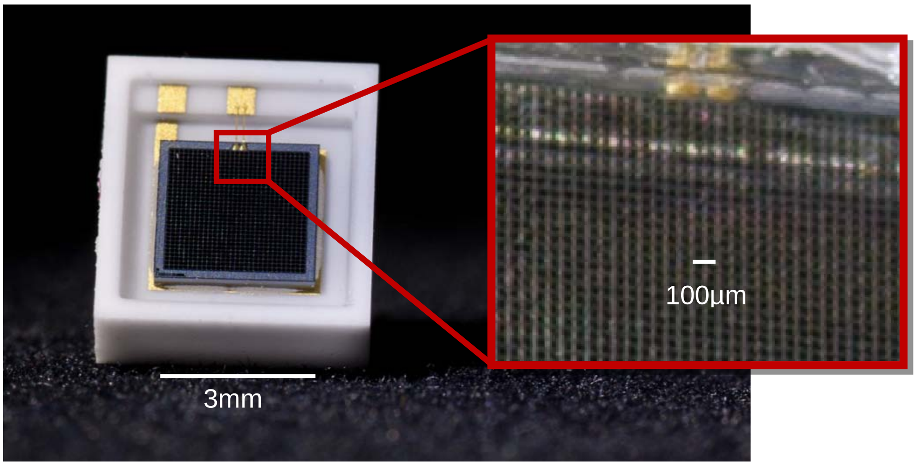

fig.2.6 Picture of a SiPMwith 100 µm / 50 µm
(3x3mm detector; Type: see appendix 5.2.2)
Left: 100 µm pixel size; Right 50 µm pixel size, magnified.

SiPMs have a fast response time and a high photon efficiency, with their built in amplification they have a high overall amplification (gain around 10^6). There are several advantages of SiPMs, namely their compactness and their insensitivity to magnetic fields. To avoid the strong temperature dependence (gain drift) and thermal noise, cooling respectively temperature stabilization is necessary.

2.3 NIM and Camac system

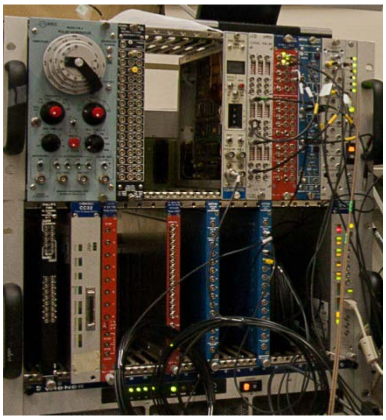

fig.2.7 Crates with NIM and CAMAC modules
The upper row shows a NIM crate, which contains signal processing devices, like pulse generator, discriminator, counter, etc.

The lower crate is a CAMAC systemcrate that is used for readout and communication withthe PC. Usual devices are TDC, ADC, etc.

1http://www.hamamatsu.com

The Wiener CC-USB system (see appendix, 5.2.5.1) was used for the **PC readout**. Since there was no USB- driver available for the 64-bit version of Windows 7, I had to use a workaround[2]. Furthermore there is the theoretical possibility of storing a command stack, executing it and storing the data in a buffer. But after some correspondence with the manufacturer, it was clear that the device would need a firmware and hardware update to use this functionality.

I alternatively installed the Wiener PCI to CAMAC System, but there is no service for 64-bit systems at all. The functionality would be the same as with CC-USB (without stack), so in all experiments, I usedthe USB module.

2.3.1 Signal processing

The main job of the NIM crate is powering NIM modules, whichare used in my experimentsfor triggering and processing of **logic NIM signals** (2 states: on and off, at defined voltages). Starting with a discriminator (see appendix, 5.2.6.5 or 5.2.6.6) a gate signal is created. It opens (state 1)when the signal reaches a specified threshold (amplitude height) and closes (state 0) after a defined time (set width with a potentiometer). (See fig. 2.8, for theory about gate creation: appendix, 5.2.1.4) This signal can be used for counting or starting a readout process in the CAMAC crate.For coincidence measurements (see 3.6, p. 26) I used an AND Logic (see appendix, 5.2.6.3), which creates a new (independent) gate signal, if all input channels are open at the same time (see following fig. 2.8).

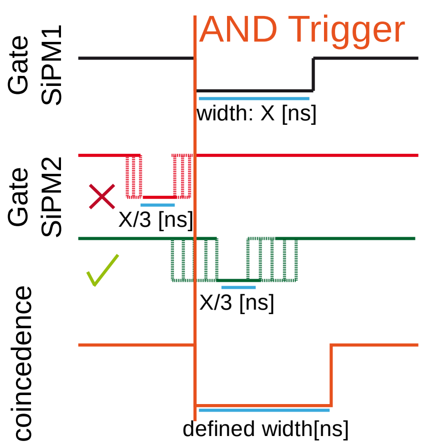

Schematics ofthecoincidence gate signal creation. Every time SiPM1 and SiPM2 are active at the same time, the AND Trigger produces a pulse of a pre-set width.

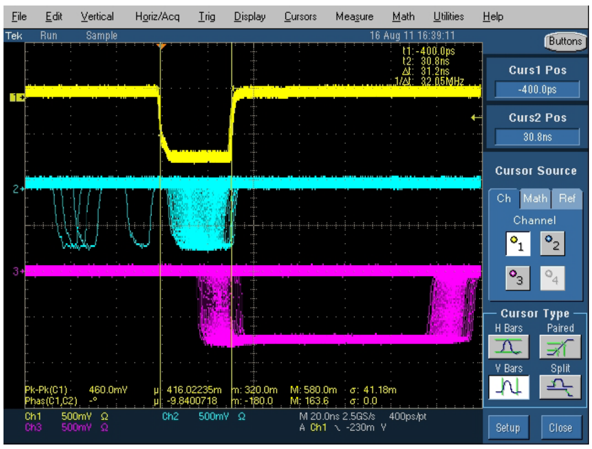

Oscilloscope screenshot of the signals. The events of the yellow channel are more periodically and are therefore used with a wider gate. Cyan is blurring and set up with a small width. Magenta is the coincidentally fired signal of the AND-logic.

fig.2.8 Theory and real signal of forming a coincidence gate (AND-logic). The signal is used to create spectra with a charge ADC.

2http://www.wiener-us.com/forums/viewtopic.php?t=50&sid=51ce27039ea043d52080ea4764b2308b or search for LIBUSB64Fix

2.3.2 ADC – Analogue to Digital Converter

Usinga LeCroy ADC (charge analogue-to-digital converter, see appendix, 5.2.5.2) I measured the charge spectra of the incoming particles. The instrumentdigitizes the analogue signal by integrating over the signal within the open gate. (Signal and gate shape, see following fig. 2.9) Since the device has a dead time the data immediately after the gate (pink signal) opens is not recorded, therefore one has to delay the signal. The manual states an opening and closing time of 5 ns as well as an internal delay of 7 ns; therefore the delay should be at least 12ns.

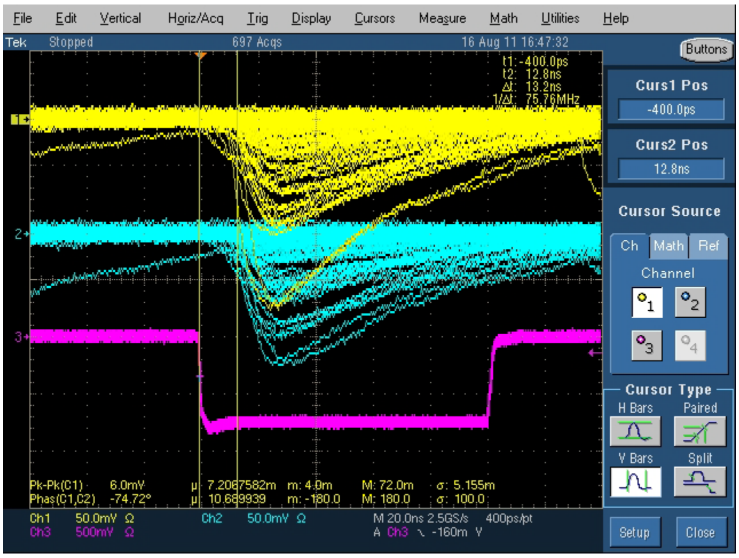

fig.2.9 Delay between ‘gate open’ and the signal for LeCroy ADC.
In respect to the internal delay plus the opening time of the ADC, the signal has to be delayed by least 12nsafter the gate opens.

2.4 Temperature measurement

In order to investigate the **changes in temperature** I used two Pt100 resistors for temperature measurements (see fig. 2.10 for the setupconfiguration). The LakeShore current source (appendix,5.2.8) provided 3mA to get a high signal. Since the absolute temperature was not important, I made no further calibrations. To calculate the temperature I used following formula (valid for temperatures less than 100°C):

$$R = R_0 \cdot (1 + aT) \qquad (1)$$

$$a = 3.85\ 10^{-3} [1/K] \ldots (linear)\ temperaturecoefficient$$

$$R_0\ \ldots\ ResistanceatreferencetemperatureT_0$$

This gives for the temperature:

$$T[K] = \frac{\frac{U\ [V]}{100\,[\Omega]\cdot 3[mA]}}{3.85\ \cdot 10^{-3}\ [1/K]} \qquad (2)$$

The behaviour of the two used Pt100 was identical, with the exception of an offset.

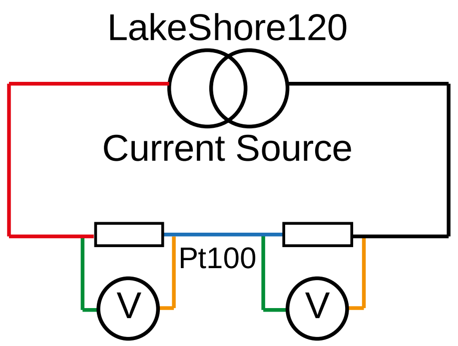

fig.2.10 Configuration of the Pt100 thermal sensors' wiring.
The thermal sensors are driven in series by a current source (3mA) and the temperature is calculated using formula (2) and measured with a voltmeter.

2.5 Temperature stabilization

SiPMs are rather temperature sensitive (gain drift, thermal noise, see 3.7.3, p. 43 ff.).To provide temperature stability and cooling, I adapted a box from a different SiPM experiment and additionally used Peltier elements and water cooling. To dissipate the heat from the warm side of the Peltier elements and also for cooling the preamplifier (it can heat the SiPM over the wiring), I connected a Rittal water cooling system (appendix,5.2.7) to the box. The **water cooling cycle** began with the Peltier cooling and continued with the preamplifier. The tubes were sealed to the box with Teflon and hose clips.

I connected the preamplifier to the water cooling with mounting it between thermal pads and aluminium. The Peltier element was sandwiched between an aluminium plate (for the thermal connection to the SiPM) and the water cooling (held by two c-clamps) and powered by a Delta electronica PSU (see 5.2.8 in appendix). The SiPM and the tip of the scintillator are surrounded by a small dedicated aluminium hood, which is thermally wired toPeltier elements aluminium plate with a copper band. To provide good thermal conduction I applied APIEZON Cryogenic High Vacuum Grease[3] on every part. Since no datasheet was available for the Peltier elements, I stepwise tested them to 1.6A at 16V, which we accepted as the safe and reasonable maximum. See fig. 2.11 and fig. 2.12 for further details.

Starting the water cooling is tricky because it doesnot have an air vent (de-aeration is automated) or a compensating reservoir; the cycle has to be filled entirely, this results in air bubbles while attaching or detaching the tubes.These **bubbles** disrupt the pump and thereforemany pump restarts are needed to draw them out. One has to make sure that they are not flowing back or the cycle will never start. If the system gets start-up aid, for instance from the water tub, it runs instantly and continuously.

3www.apiezon.com

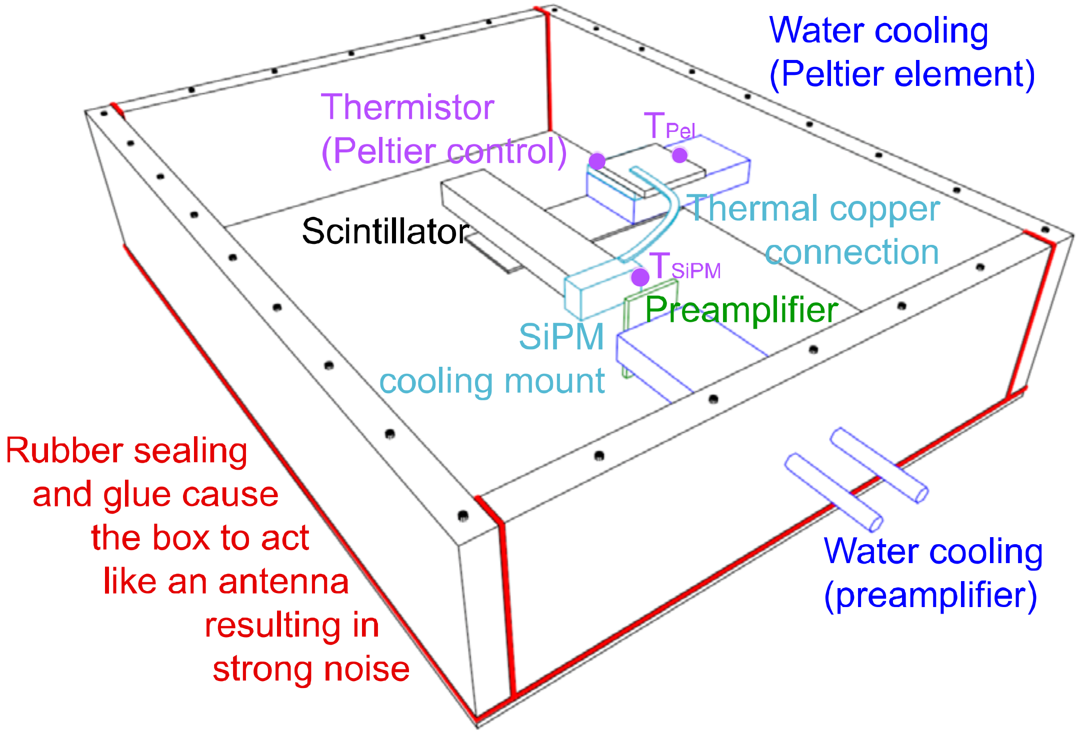

fig.2.11 Schematics of the evacuated, light tightchamber with temperature controlling and stabilization for the SiPM.

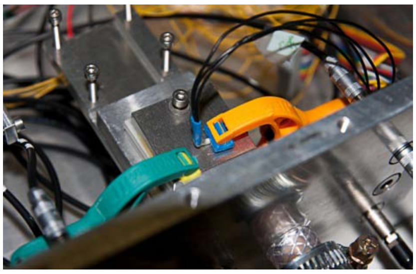

Peltier element and PT-100 are mounted with c-clamps.

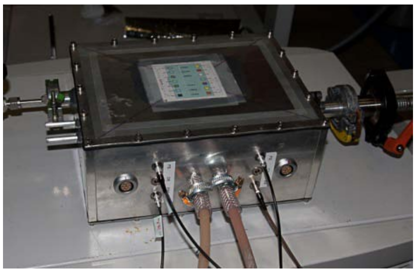

Evacuated and light tight test box.

Problem: ice, if not evacuated. could cause damage through water

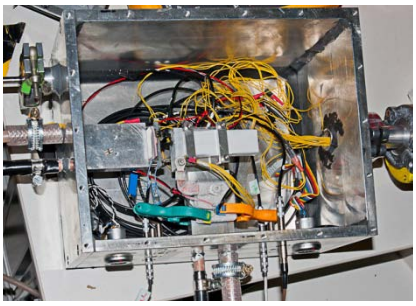

Opened box, top view.

fig.2.12 Pictures of temperature controlled/stabilized setupin a light tightboxfor testing ofthe temperature dependency of the detector.

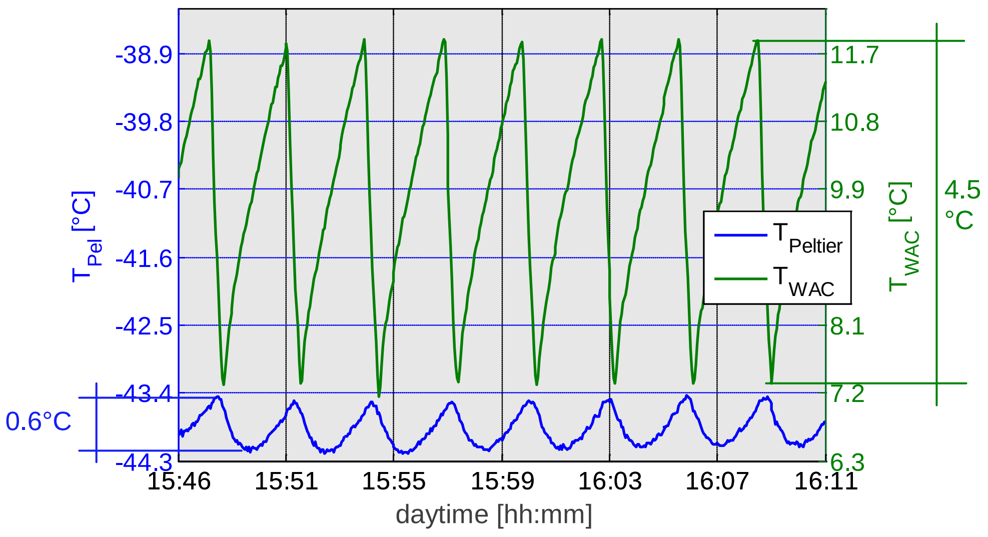

fig.2.13 Oscillation ofthe water cooling system and Peltier element.
(2°C threshold, 10°C set point; no Peltier cooling)
The cooling cycle is controlled with a set point and a threshold. If the set range is exceeded, the water is cooled (green line). One can see a temperature change on top of the aluminium plate – that is positioned above the Peltier element – of up to 0.6°C.

After some temperature measurements it turned out that the water cooling system is varying by more than 4°C. When set to 10.5°C with a threshold of 1.5°C the water is cooled from 12 to 7.5 which has an impact on $T_{Peltier}$. This oscillation is even visible at T_{SiPM} (see fig. 2.13).

To avoid these oscillations a Peltier element control unit (MPT-5000,see 5.2.7 appendix)should compensate the fluctuations of the water cooling. It is regulated with a thermistor (thermal resistor),which I mountedon top of the Peltier element. One can set the temperature level with aset pointthatregulates thePeltier current.

To ‘synchronize’this device with the water coolingI set the local set point to zerolevel at water cooling temperature, so itwould be stabilized automatically.A lower temperature can then be set in a LabView program. (Compare the upper chart in fig. 2.14)

As can be seen in fig. 2.14 (lower charts), the result of the stabilization is marginally better (0.4°C instead of 0.6°C). The SiPMs temperature is oscillating and has an amplitudeof around 0.1°C. I read the data using a NI USB data acquisition device (see 5.2.9).Comparing the results with cooling switched on and off, one can see thatit is oscillating in each case. Therefore we have to use an acquisition device with higher resolution for future experiments.

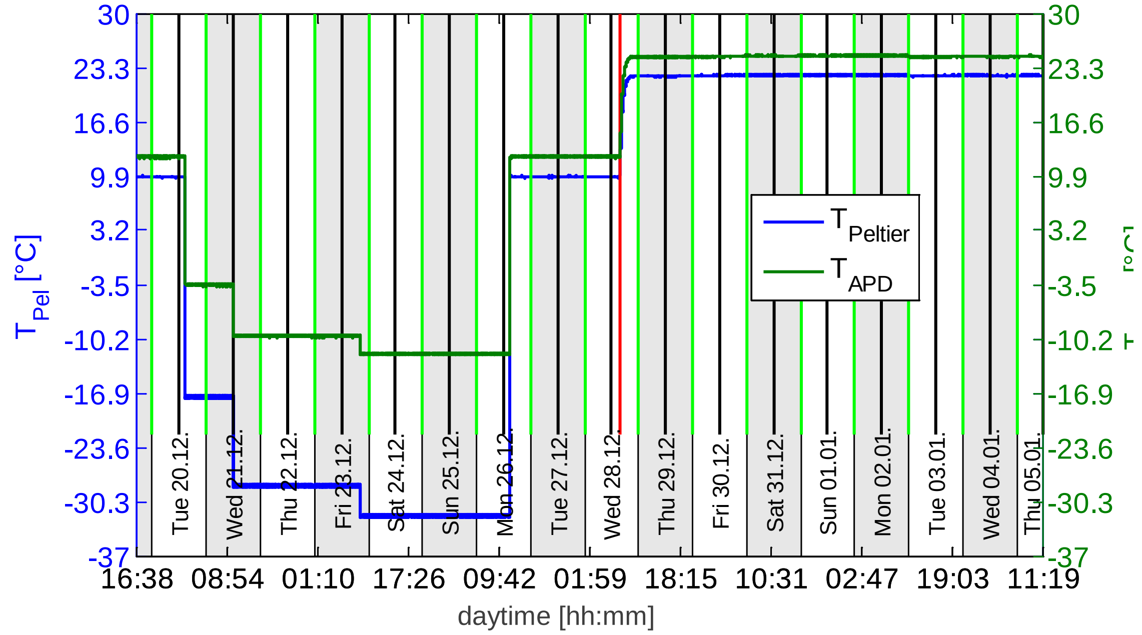

Long term temperature stability test withvarious MPT-5000 set points. The red line indicates cooling shutdown

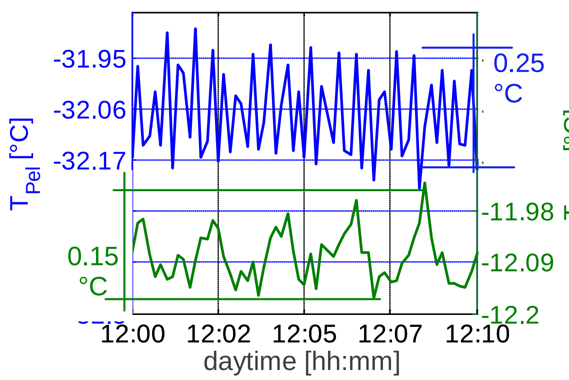

Oscillations zoomed in. (cooling active)

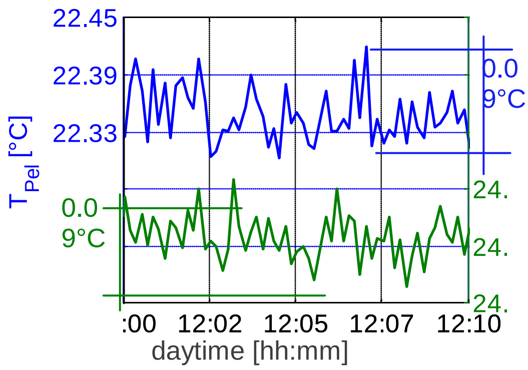

Oscillations zoomed in. (not cooled)

fig.2.14 Test measurement, of the temperature stabilization, with a Peltier element.
(stabilized with MPT-5000, acquired every 10s)
Blue: Peltier elements temperature.
Green: Temperature of the SiPM. (Higher temperature due to the connectionwith 7 cm long copper band)
The lower graphics are zoomed-in areas with cooling switched on (left) and off (right).This proves that the fluctuations are caused by aninsufficient resolution of the USB DAQ. Further the regular oscillations of the SiPM with cooling switched on suggest that the preamplifiers water cooling is influencing T_{SiPM}

3 TESTING

3.1 SIGNAL AND NOISE

Since the light collectionthroughthe aluminium wrapping(see 3.3) was not as good as through Teflon (using a Na-22 source), I only used latter in future measurements. In a rudimentary setup I establisheda communication with the Camac system andtested the **effects of different thresholds** of the discriminator on the signal. I used size Ascintillator. (See p.8)

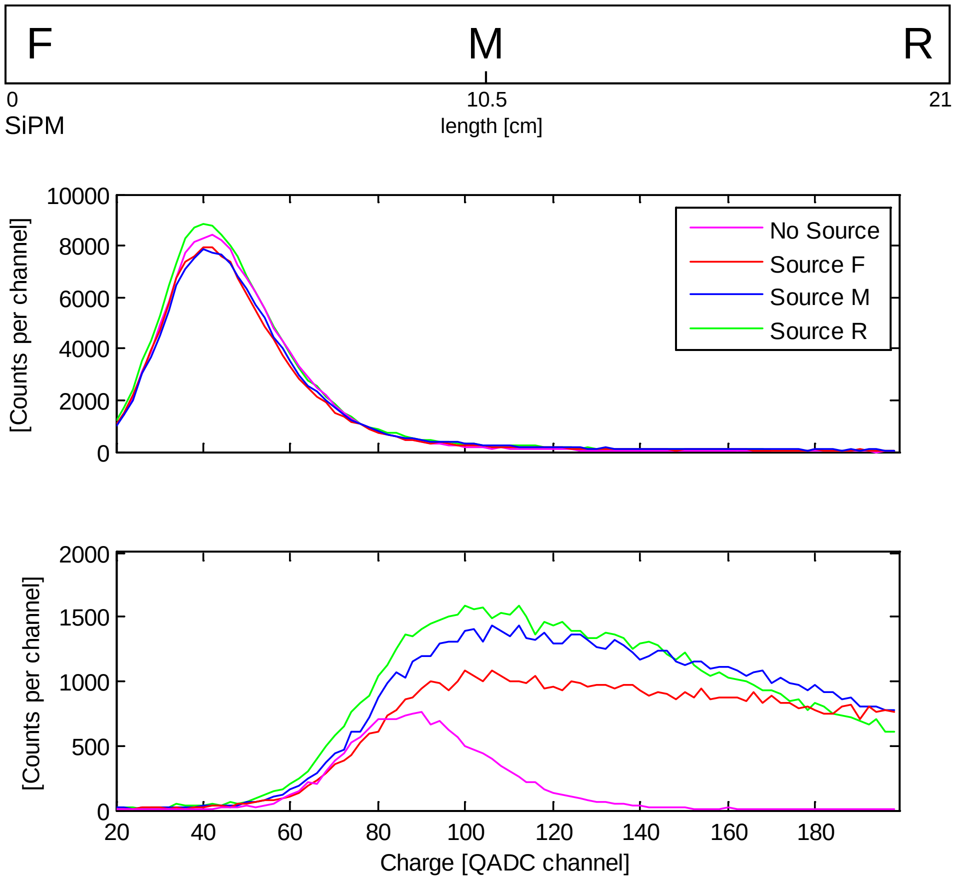

fig.3.1 Charge ADC spectra attwo different thresholds (40mV (top) and 80mV (bottom))
Four states: Noise, Na-22 source near the SiPM, in the middle and at the other end of the scintillator. (SiPM1, 70.76V, 120 s)

fig. 3.1 shows that at low triggering levels the ADCs **dead time rate** is too high, which results in non-predictable results and a noise like spectrum.

3.2 Collimation of the Na-22 source

The radioactive source causesa signal with a high rate and emits radiation in a wide angle that, for positioning tests, is not useful.Toimprove this, collimation is necessary. I tested several small ‘apertures’ of different materials without any measurableeffect. To lower the intensity, it is important to **increase the distance** between the source and scintillator, so a small brass‘tube’with 4.5cm diameter (and an even smaller inner radius of 1mm), a height of 5cm and a 1cm deep inlet for the source(diameter 2.6 cm) was made by the workshop.

Scattering within the brass material is smearing the signal to lower energies (see fig. 3.2). This signal is not usable for spectroscopy, the focus is better for positioning experiments.

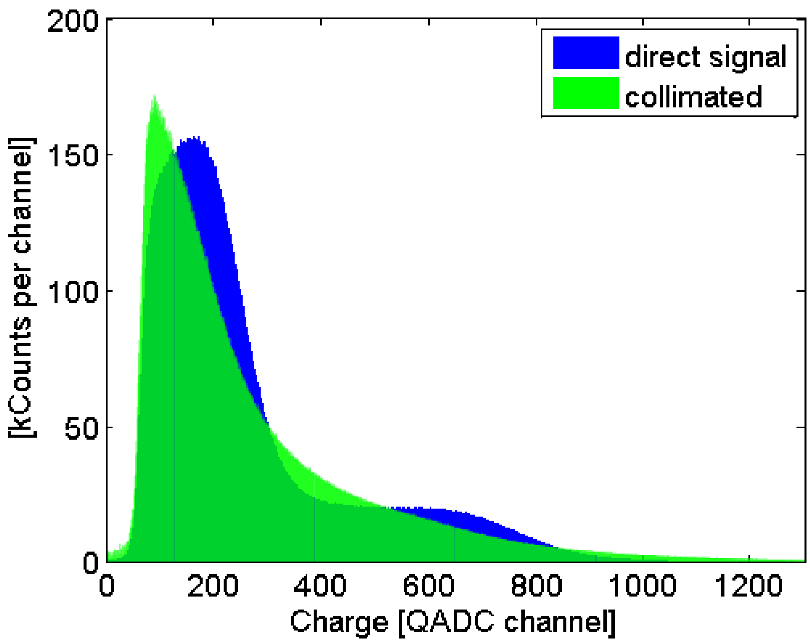

fig.3.2 Signal comparison of collimated and direct source signal. The collimator is smearing the spectrum because of scattering in the brass material. (24h, Threshold -60mV, U_{BIAS} = 70.87 V)

3.3 Counting rate distance dependency

To get an idea of the measurement performance – depending on the position of the Na-22 source –with one SiPM mounted at one end of a 20cm long scintillator (size A, see p.8), I used a Picotest Counter(appendix, 5.2.9) to measure the counts per second. I set the trigger to -400mV and the counts were averaged over 100 values.Then, as stated in the datasheet (see 5.2.1, appendix), Iapplied the SiPM bias voltage. The data shown in fig. 3.4 is averaged over 15 values from every position I moved the Na-22 source (appendix, 5.2.10) to. (Starting with the radioactive source positioned at 12mm, moving it to the end of the scintillator in steps of 2.5cm. I centred the source window to half-height (1cm)of the scintillator).

To see if the **wrapping material** makes any difference I measured with two scintillators, one in aluminium foil and surrounded by isolating tape and the other wrappedwith 2 layers of Teflon tape. I placed them setup in a carton box lined with light tightening felt paper and marked spots on the outside for positioning.(See fig. 3.3)

One of the insights drawn from the experiment was that the signal with aluminium wrapping was smaller and produced less counts, because the photons are not reflected as good as with Teflon wrapping.Another interesting thing is that the countsclose to the SiPMare around 20% less than a half step (1,25cm) further and the overall performance is decreasing almost linear till the end (at 20cm) to about 25% of the maximum. (See fig. 3.4)

Signal with Teflon wrapping

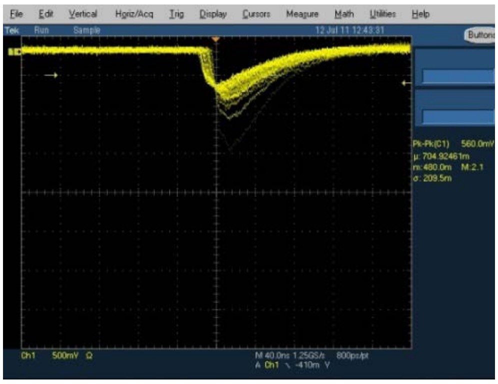

Signal with aluminium wrapping

Setup: scintillator held by cellular plastics

Positioning scale and Na-22 source

fig.3.3 Signal comparison of different wrappings and pictures of the measuring setup.

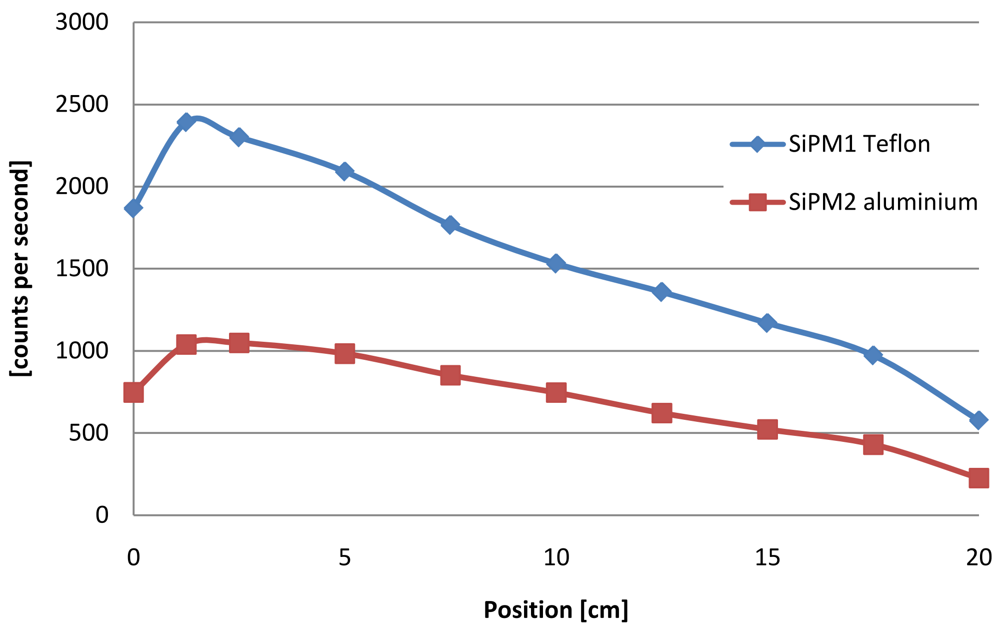

fig.3.4 Rate dependence of different source positions along the scintillator. I tested two different scintillator wrappings (aluminium, Teflon);wrapped aroundsize A(see p.8) scintillators. The attenuation effect on both detectors is similar, but aluminium wrapping produces a weaker signal. (Positrons from the NA-22 source are blocked.)

3.4 Charge ADC spectra at different Na-22 source positions

In this experiment I tested thelight producing efficiency of a scintillator as well as itsdetection withSiPMs(mounted at both ends). I measured the detection at **11 different positions** (see fig. 3.6, top)by placing a Na-22 source.For the test I used twodetectors (both size Ascintillators (p. 8) wrapped in Teflon, aluminium and black isolating tape), onewith SiPM1/SiPM2mounted and another one with SiPM3/SiPM4mounted. The aperture of the collimator (1mm) is rather small compared to the size, so the positioning was rather inexact.I set the bias voltage to the value given in the datasheet, and adjusted the threshold to -60mV (compare3.2).

To create a reference forthe positions I used the data from a 24h test with the source in mid position (plotted as ‘SM’ in fig. 3.6). I cut the data into 100k bundles (sum up) and with this defined starting points for the other positions.

One can see (in fig. 3.5) that the efficiency/spectra height is around 20% less near the edges (A1/C1, A4/C4).

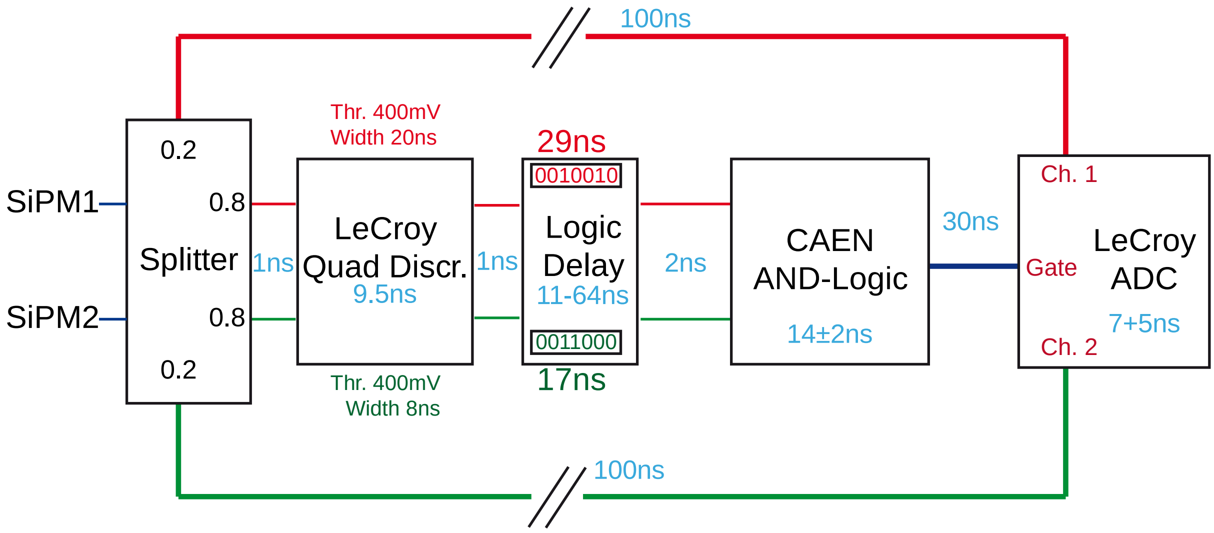

fig.3.5 Configuration of energy spectra measurement setup at different source positions
(see next fig. 3.6, top)
The ADCrequires a gate (in which the signal has to appear, delayed by 13ns), therefore the signal is split (80/20%, see 2.3.2, p. 14).

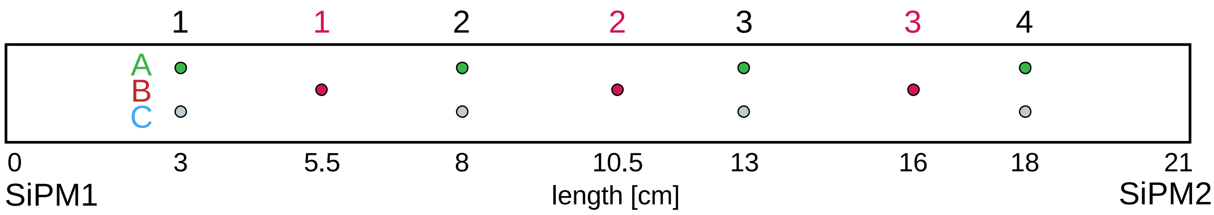

Positioning schemeof the source for the graphbelow.

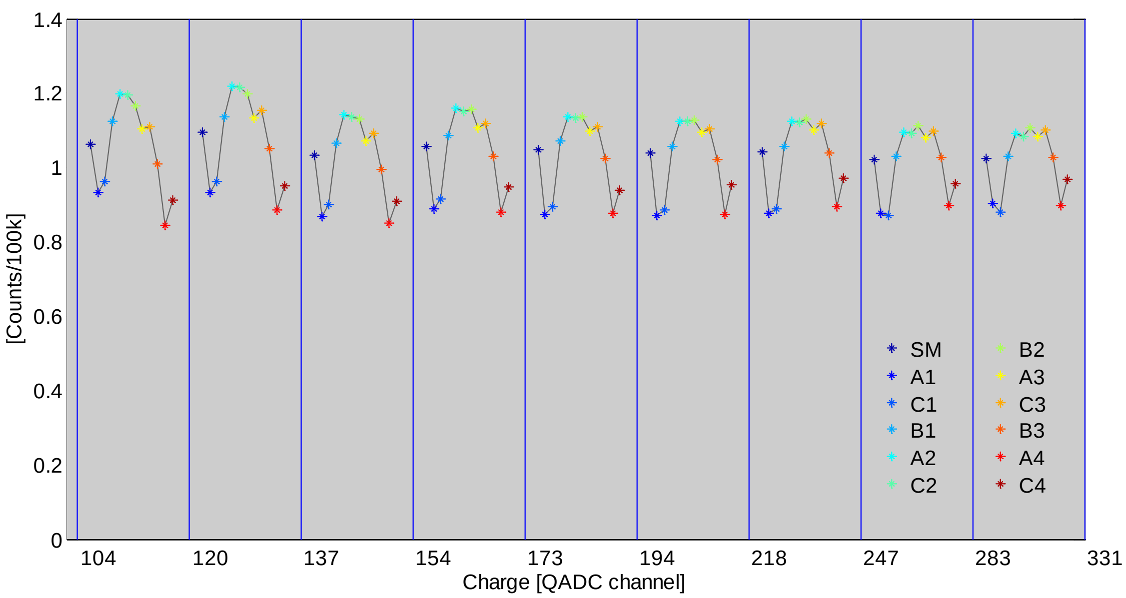

fig.3.6 Position dependenceof the charge ADC spectra (normed)
The x-axis shows the beginning channel number of 100k chunks (defined with a normed 24h measurement(SM) with source in B2 position)
There is a tendency that the efficiency near the ends of the scintillator is 20% less than in the middle. (A1/C1, A4/C4)

3.5 SiPM BIAS VOLTAGE DEPENDENCE

The questionof the **influence of the bias voltage** on the signal came up. Since the dioderequires a minimum voltage to work, thisis a limiting factorat the lower end of the testing parameters. Furthermoreif the supply is too high it would destroy the semiconductor. ThereforeI chose a 1.5V wide area, starting from a hardto triggersignal to anoisy and high rate signal. (measured in steps of 0.1V for 1min each) The tested SiPM7 was mounted on the same scintillator (Size A, p.8)as in3.6.2 (p. 27).

As can be seen in fig. 3.8 the **spectral shape is transforming** from a peak to a broad meaningless form.The area 70.9-71.2V looks most promising and is in the range of the voltage stated in the datasheet. (71.19 V at 25°C)Since the temperature is a highly influential factor (see 3.8, p. 50) and (according to this chapter) even small changes of the bias voltage deform the spectra, the operating voltage should be well controlled and stabilized.

The counting rate increases with higher voltage which the ADC cannot handle, therefore the setuptakes care of the ADC's **dead time**, which is realised with a delay line veto of the discriminator(fig. 3.7).The counting rate is cut at a maximum of 8600 counts/10s. The source is collimated and positionedin the centre of the scintillator while a light tight carton box covered the setup.

Counting rate overview [events/10s]:

70.3V	0.1k	71.1V	8.3k
70.4V	2.8k	71.2V	8.4k
70.5V	6.3k	71.3V	8.4k
70.6V	7.3k	71.4V	8.5k
70.7V	7.6k	71.5V	8.7k
70.8V	7.9k	71.6V	8.6k
70.9V	8.1k	71.7V	8.6k
71.0V	8.2k	71.8V	8.6k

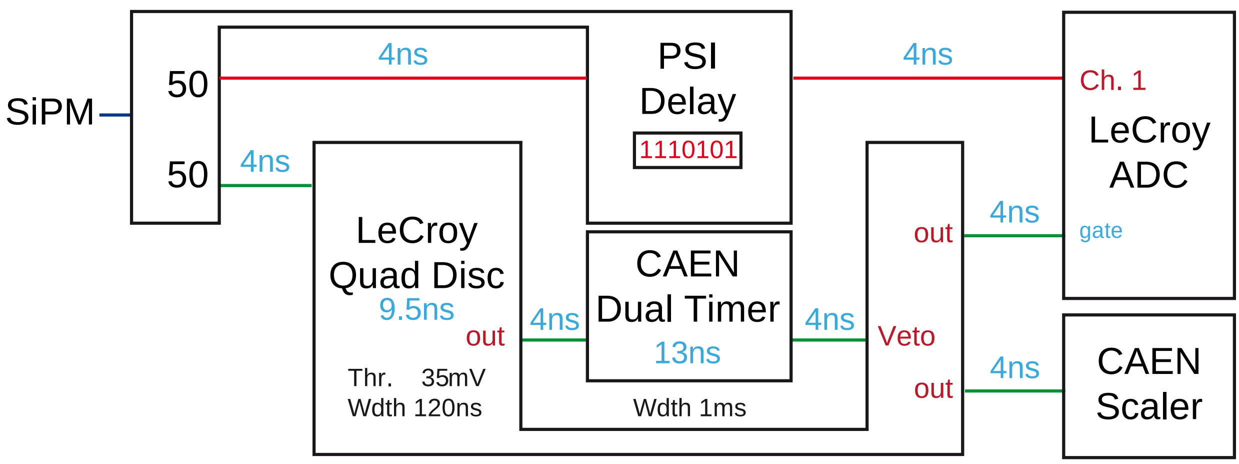

fig.3.7 Configuration of the vetoed ADC for comparison of different SiPM bias voltages.
The discriminator is vetoed for 1ms after every event to avoid the ADC's dead time.

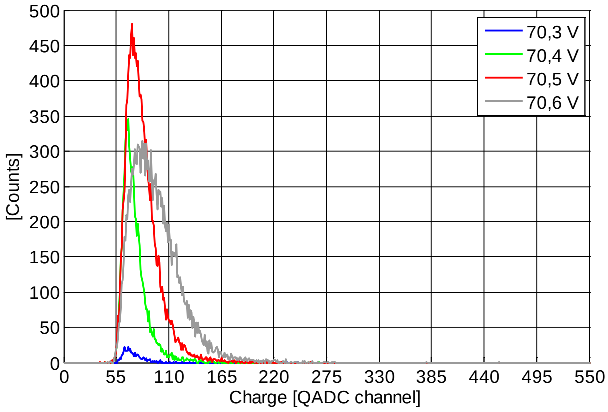

Bias adjusted close to noise level. This results in insufficient amplification.

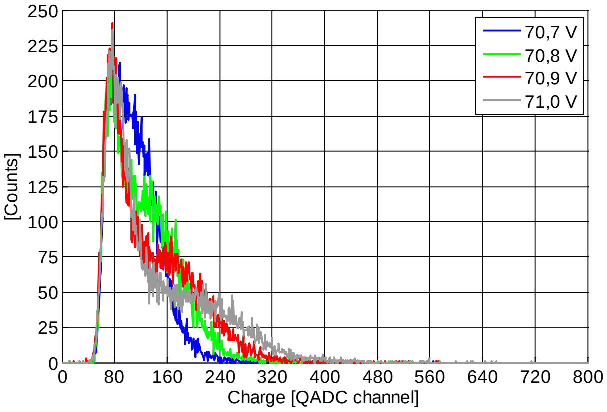

Working conditionslie around the expected 71V gain.

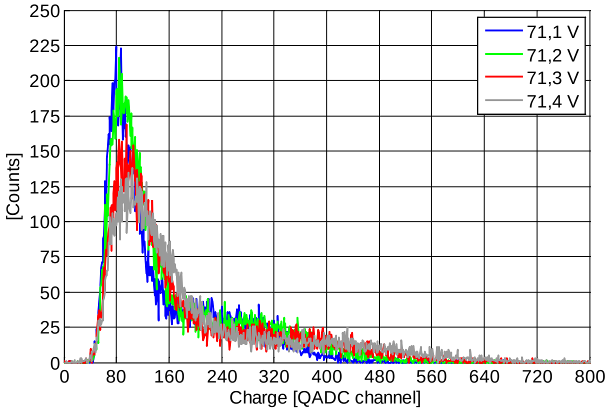

Crosstalk starting from 71.3V.

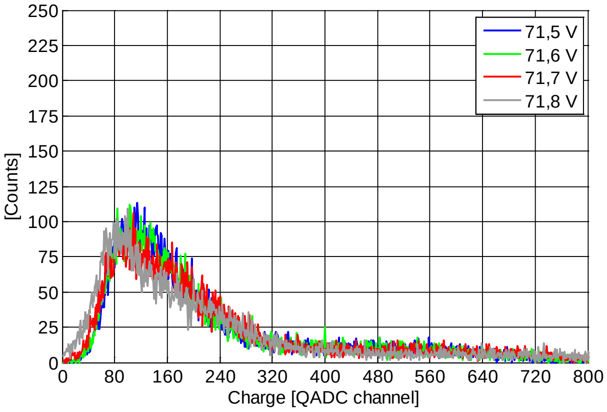

No difference at biases beyond 71.5 V

fig.3.8 ADC channel spectra at different SiPM bias voltages.
(The Voltages given in the legends.SiPM7, 1min, thr. -35mV)
The diagram shows that the ideal bias voltage is between 70.9-71.2V (at room temperature). This range has to be considered when specifying the voltage/current of the final setup, with respectto the temperature dependency.

3.6 DETECTOR TIMING MEASUREMENTS

The study of the timing performance is another big part of this thesis, because a good timing opens interesting possibilities and helps to make decisions on the setup. One of the main questions is if it is possible to **localizeparticles** with two SiPMs mounted on one long scintillator or better use 2 (half its size) scintillators with one SiPM each and just have the information if it has hit the upper or lower one.

Of further interest is if the detectors are fast enough to recognize '**window stops**' (K^-thatare stopped in the entrance window of the target cell). The whole SIDDHARTA-2 setup will be triggered with a start signal from the accelerator and these stops would occur immediately after it.

3.6.1 TDC LINEARITY CHECK

To make sure that all further measurements are valid, I measured the TDCs (appendix,5.2.6.5) linearityover the full range with no changes to the setup. I used a high precision delay/pulse generator (appendix,5.2.10) and set the channels to 50Ω inverted NIM signal (T0 to common start, A to stop ch1) with a frequency of 100 Hz and increased the delay via IEEE interface in LabView.

LabView acquired the signal for 1s in steps of 0.1ns and the diagram (fig. 3.9) shows the maximum, minimum and mean value. Except for a few outliers (electronic channel errors) the linearity is given with a slight offset and some distortions at lower timings. Furthermoredata could not be acquiredontimings higher than 96ns.Formula(3) shows the linear equation of the module.

$$y = 0.9908 \cdot x - 3.2357 \tag{3}$$

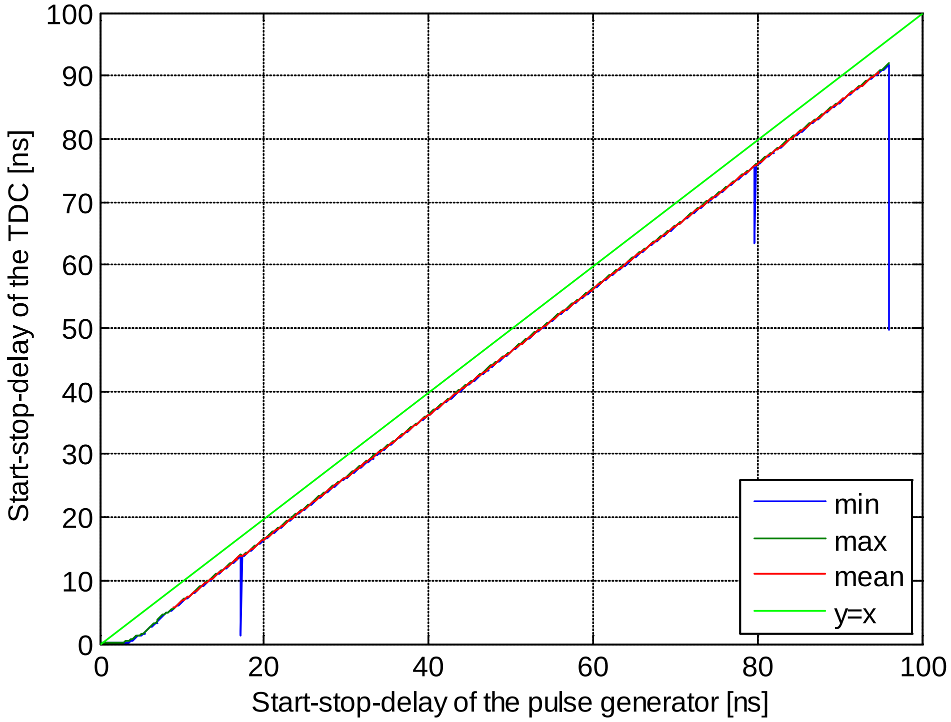

fig.3.9 TDC linearitymeasured with high precision pulse/delay generator
The graph shows minimum, maximum and mean values. Except for a few digital errors their distance is in a range of 11±10 TDC channels.I set theTDCs resolution to 100ns with a range of 12 bit (≈25 ps per channel).

3.6.2 Positioning withcoincidence trigger

For timing resolution measurements I mounted 4 SiPMs on 3 scintillators. To generate a coincidence start signal I attached SiPM1 and SiPM2 each on one small scintillator (Size C, p. 8) and wrappedthemwith Teflon, aluminium and isolating tape. AfterwardsI fixed these **triggering scintillators** on an aluminium U-profile(seefig. 3.10), together withthe preamplifiers.The SiPMs are powered with the voltage stabilized supply (appendix,5.2.1.2).

SiPM3 and SiPM4 I attached to each end of a big (Size A, p. 8) scintillatorand powered themwith the Keithley PSU (appendix, 5.2.8).

To provide some space for moving the U-profile, I placed the scintillator on small blocks of aluminium and another pair of blocks upon it to fix the preamplifiers (fig. 3.10). Furthermore I taped the cables (because they are very stiff and caused the scintillator to tilt) on the desk to make sure the setup does notmove during the experiment and while adjusting the U-profile's position.

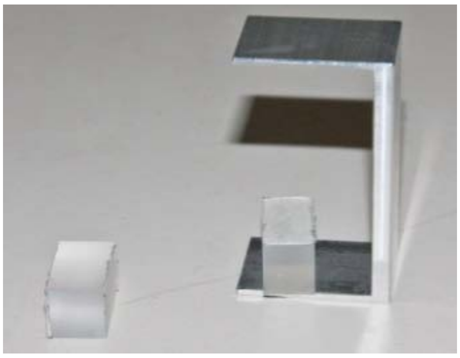

U-profile and triggering scintillators

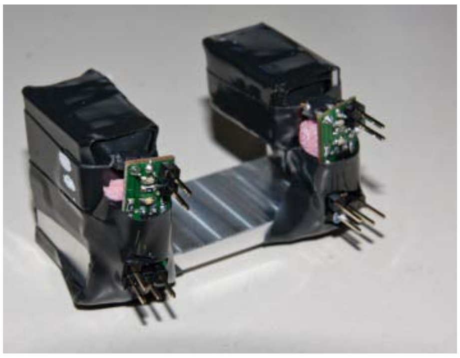

Finished coincidence trigger.

Setup (side view)

fig.3.10 Pictures of thetiming positioningtest measurement setup.
The U-profile is moveable and SiPM3 respectively SiPM4 are providing the coincidence start signal. Due to the rather stiff cables it was not possible to move close to SiPM3 that is why the experiment was repeated (compare fig. 3.12, top).

For test measurements I placed the Na-22 source (appendix,5.2.10) between SiPM1's and the main scintillator. I used the non-collimated source because when the collimated source was placed on top of the U-profile there were only 85 events after an overnight test. This is confirmed to be cosmic radiation in later experiments.

With a NIM Counter (see 5.2.6.4) I searched for the ideal source position to find a solution for this problem.(Counted over 10s,collimated source placed on top of the U-profile (Position 3, see fig. 3.10)).

<table>
<tr><th></th><th>U-profile</th><th>U-profile
180° turned</th><th>Coincidence</th></tr>
<tr><td>SiPM1 [counts]</td><td>1460</td><td>440</td><td rowspan="4"><15</td></tr>
<tr><td>SiPM3 [counts]</td><td>1350</td><td>similar</td></tr>
<tr><td>SiPM4 [counts]</td><td>1320</td><td>similar</td></tr>
<tr><td>SiPM2 [counts]</td><td>400</td><td>1400</td></tr>
</table>

After some more researchthe final resultwas placingthe Na-22 sourcewithout collimation between the upper and main scintillator.One has to be aware that the source output is not the same on both sides:

	Foil ↓	Foil ↑	Coincidence
SiPM1 [counts]	150k	64k	>100
SiPM3+4 [counts]	30k	50k	
SiPM2 [counts]	13.5k	19k	

The following fig. 3.11 shows the setup of the signal processing including a schematic of coincidence gate creation.

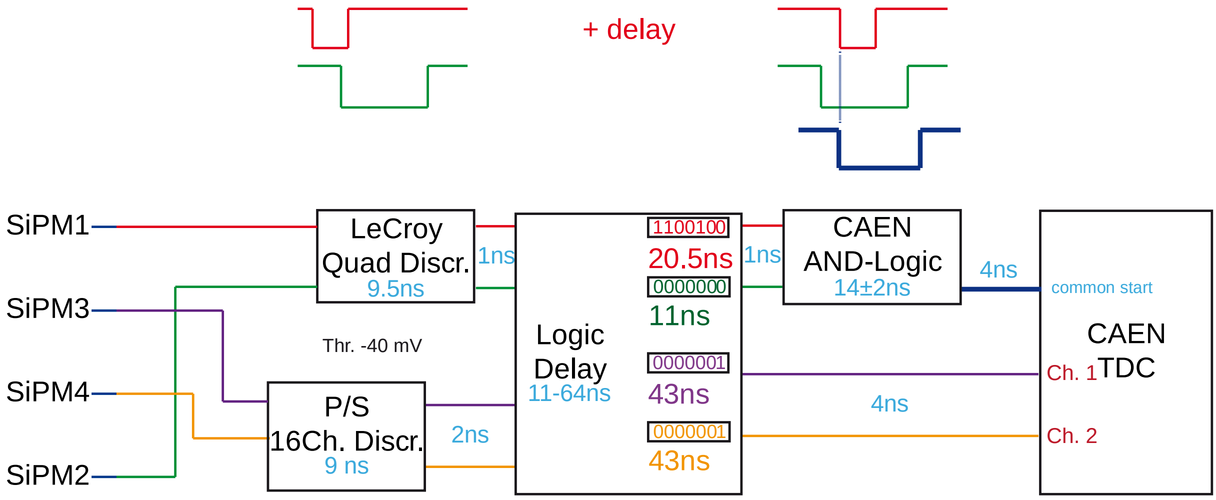

fig.3.11 Configuration of the coincidence setup for positioning test. The P/S discriminator uses one threshold for all channels and is connected tothe signal of the main scintillator. The AND-logic creates the coincidental start signal for the TDC. (See2.3.1 for signal processing)

It was difficult to measure position 1 because of the rigid cables, so I rotated the U-profile about 45° at this position and repeated the whole measurement with the U-profile on the other side (resulting in the same problem at position 5; fig. 3.12, top). The data analysis (see graph in fig. 3.12) shows that it is possible to get an idea of the position of the source (right/red plots).

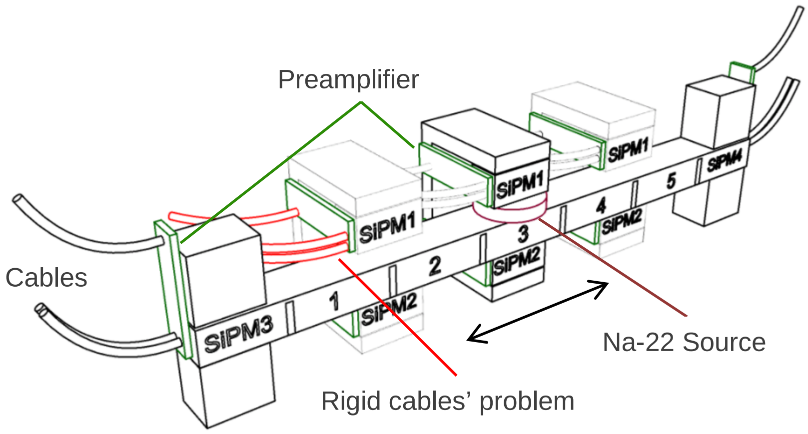

Schematic setup:moveable u-profile with SiPM1/2 for the coincidence start signal.Measurements at5 defined positions.

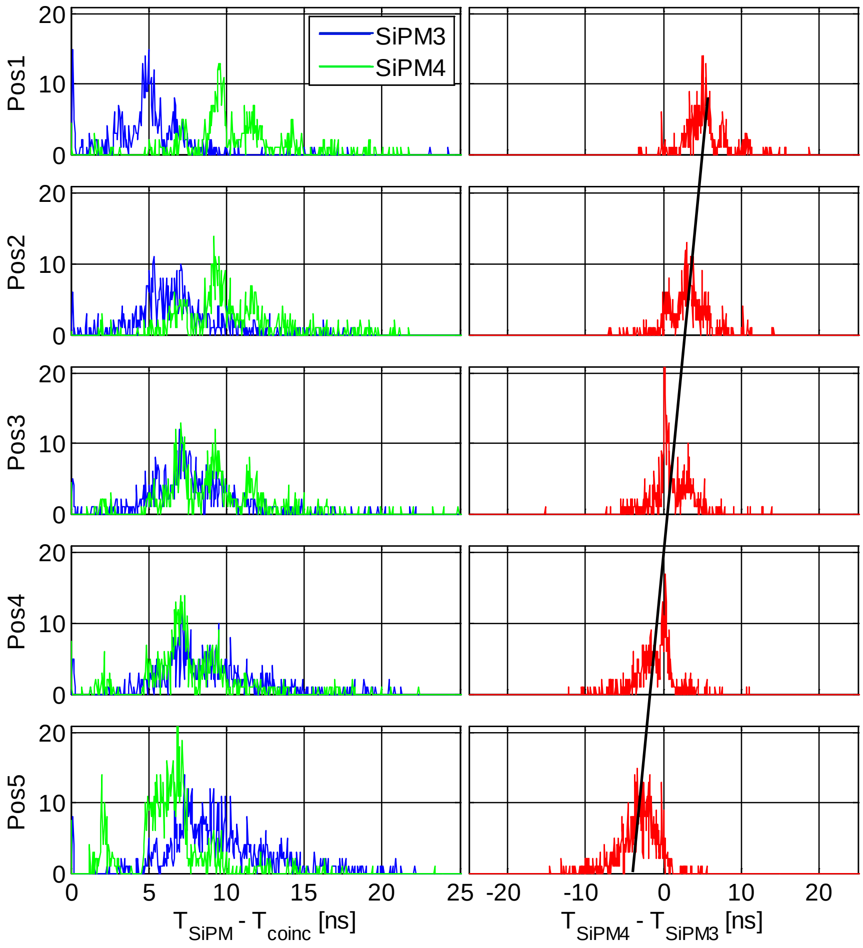

fig.3.12 Time difference spectra at five source positions.
The left column shows the timingof the SiPMs separately. (thr. -40mV, 1h)While the right shows SiPM4subtracted by SiPM3. One can see a tendency inthe difference between position 1 and 5.For positioning 8ns can be expected between the outer positions. The distortions are due to reflections in the scintillator originating from the source.

3.6.3 Long-time measurement with cosmic radiation

In a measuring period of about 30days, LabView collected as much data as possible.The setup consisted of a TDC and an ADC (see 2.3, p. 12) as well as a National Instruments DAQ (appendix,5.2.9) to acquire the temperature (see 2.4, p. 14). The LabView program crashed several times due to a bug connected to the USB DAQ. Since even a built in data acquisition software (NI DataLogger) did not collect useable data, an error inthe code was overlooked and only fixed later.After the period has elapsed, the result showed about 8800 trigger events within 30 days. This small number results from the fact that the coincidence scintillators have a very smalldetection areaand the cosmic radiation had to pass through both of them.fig. 3.13 and fig. 3.14 show the setup and signal processing. fig. 3.15 shows interesting statistics about cosmic radiation as well as the TDC and the charge ADC spectra.

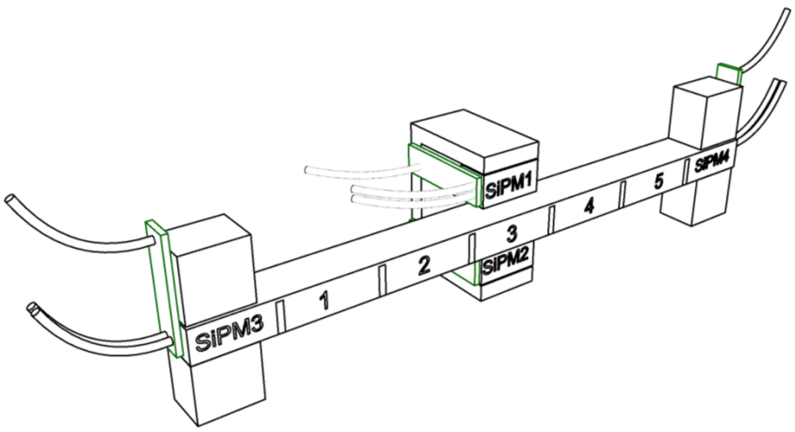

fig.3.13 Long-time measurement assembly. (Cosmic radiation)
For this measurement, I left the u-profile at position 3 because a low particle rate was to be expected.

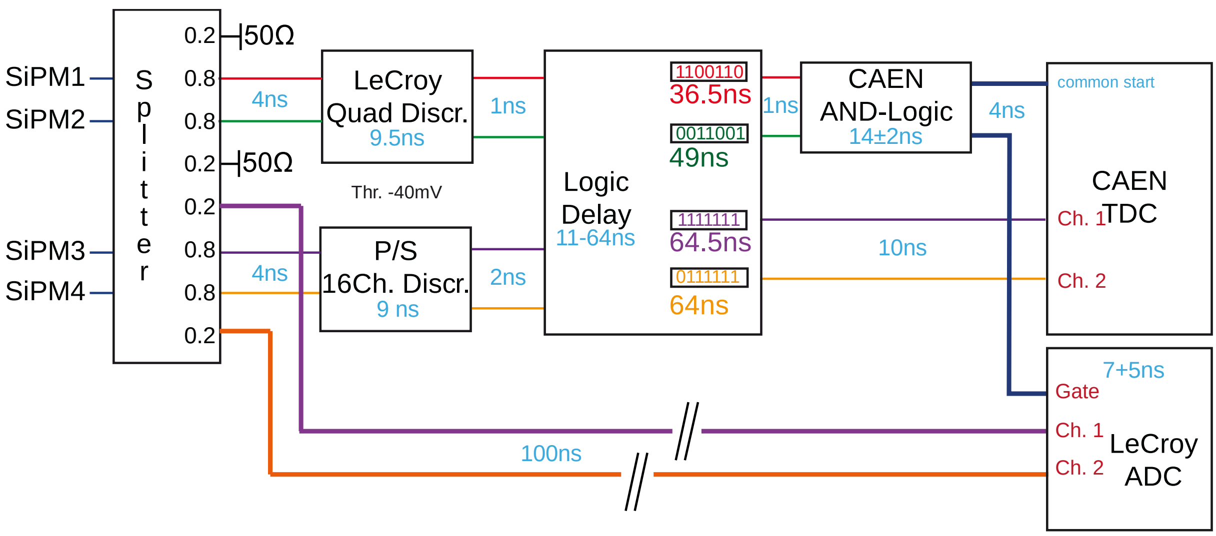

fig.3.14 Configuration of the long-time measurement (with cosmic radiation).
Since the basis should be the same for the coincidence and measuring signal both are split, thereforeone has to keep in mind that the trigger is higher than it appears. Coincidence through the AND-logic provides the start signal for ADC and TDC.

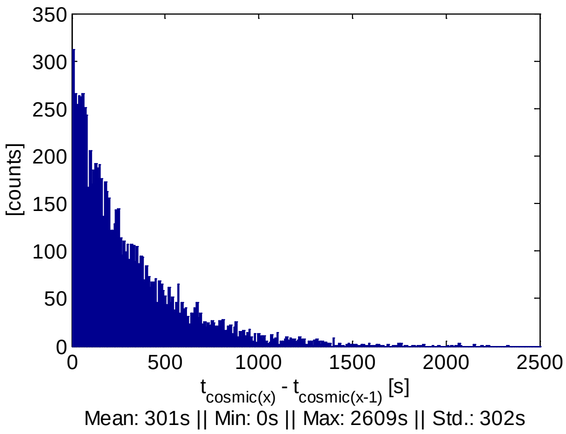

Cosmic radiation arrival time distribution.

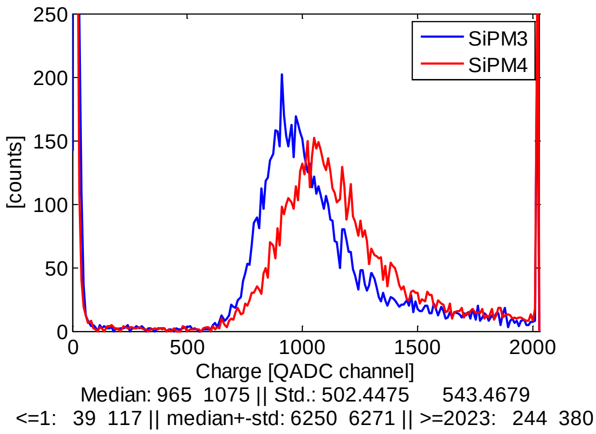

QDC spectra of cosmic events.

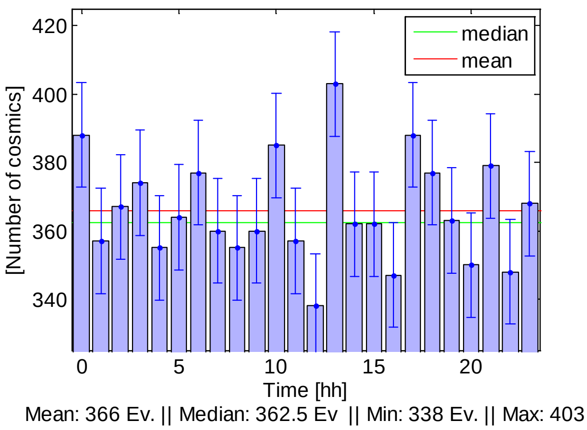

Average events for each hour (0-23 h) over 30 days.

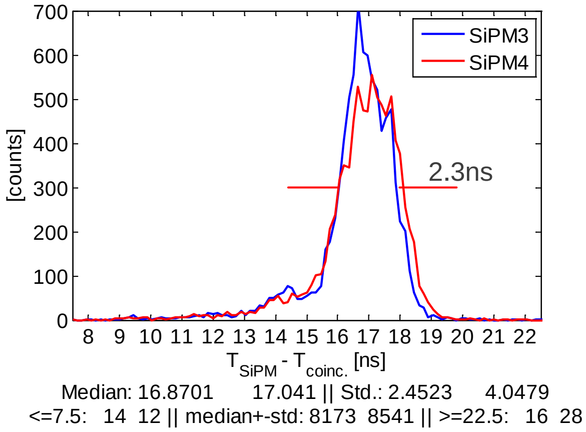

Coincidental timedifference of the SiPMs.(TDC scale 100ns)

fig.3.15 Datasummary of the long-timecosmic radiation measurement. (4 weeks, coincidence in mid position, threshold: -40mV)

3.6.4 Timing at different SiPMsurface positions

For the next experiment I prepared athicker scintillator (Size D, p.8)witha quadratic cross-section and equipped it with four SiPMs (50 µm pixel size) at different front end face positions (see fig. 3.17, right; SiPMs:appendix, 5.2.1:SiPM5 ff.) To measure the timing, I positioned one of the small scintillators from 3.6.2 (Size C, p. 8) on top of the detector.ADC, TDC and a NIM-countercollected data triggered bycosmic radiation (configuration, see fig. 3.16).The signals amplitude was too low therefore I needed apreamplifier to getatrigger-able signal on the oscilloscope. The amplification distorted the spectrum, so the ADCreadout was useless.The graph in fig. 3.17 shows the timing results. The width of the peak is around 4 ns which is approximately twice as wide as with a size A scintillator (see fig. 3.15).

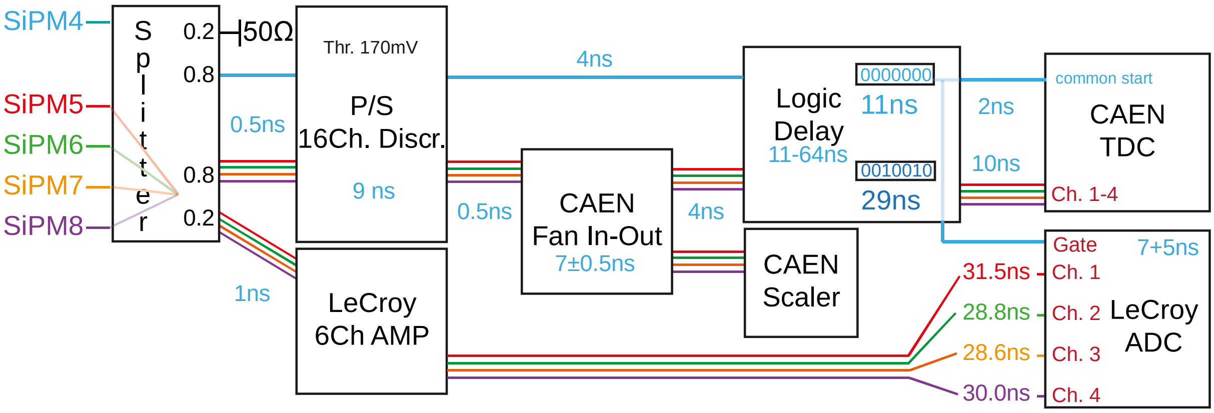

fig.3.16 Configurationof themeasurementof different SiPMfront end face placements.
The size Cscintillator with SiPM4 mounted is positioned above the tested one (size D, p. 8), serving as trigger for TDC and ADC. First tests showed that the spectrum of the ADC is distorted because of the amplifier. Therefore the data could not be acquired as it wasdone in former experiments.

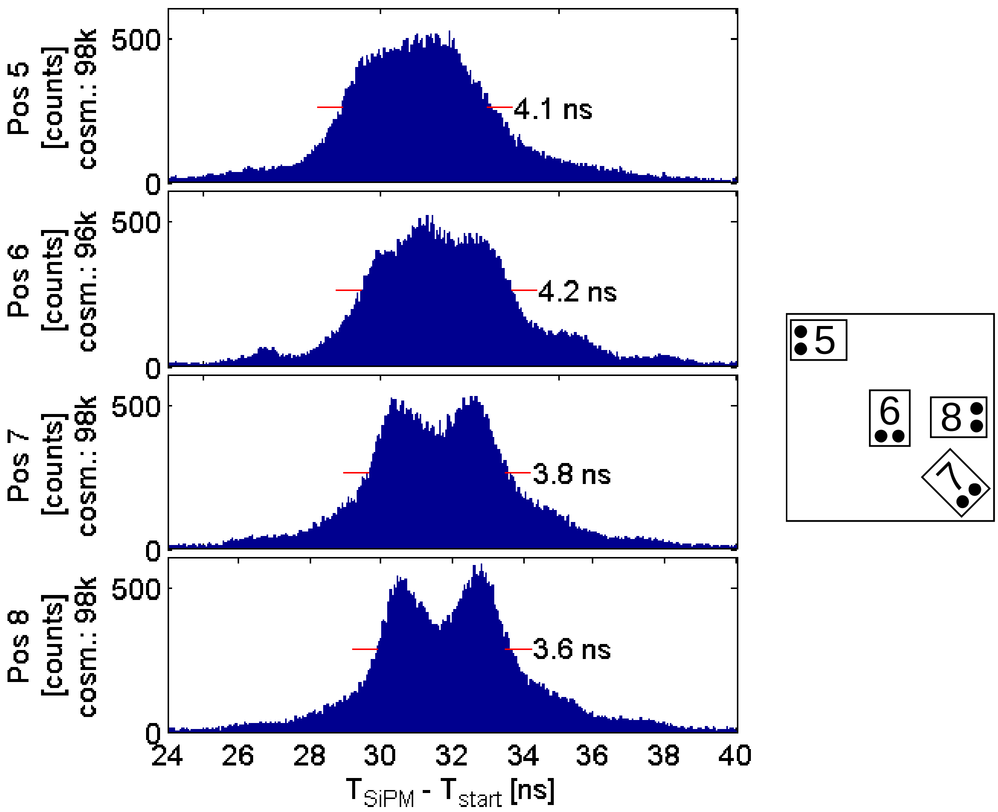

fig.3.17 TDC spectra of different SiPM front end face positions.
(cosmic radiation, 6 days, Thr. -25mV)
Point of interest in this experiment was measuring the TDC data of different front end face positions (see right scheme). The widthsshow no large difference, but a structure, due to reflection, is visible. We assume that this is caused by impuritiesin the scintillator material.

3.6.5 Timing of size E scintillator

As next step I polished only the front end faces of a large scintillator (size E, p. 8). Because of the dimensions and several impurities/geometrical issues (see fig. 3.18), it was not possible to polish and wrap it as tight as in the usual process (see 2.1, p. 7). I mounted SiPM9 and SiPM10 in the centre of one front end face.

Non quadratic cross-section with a jet like inclusion in the centre.

The surface is clear but uneven like formerly molten plastics.

fig.3.18 Impurities and geometrical issues of size E scintillator.

For triggering I used the scintillator from 3.6.4 (SiPM6, size D, p. 8).Thelight collection of this huge detector is comparatively low, because the large cross section area is not covered completely with SiPMs; respectively no light guide was installed. The counting rate with the source positioned at different spots gives a ratio between SiPM9 (same as SiPM10) and SiPM6 (upper triggering scintillator) of about 1:400 (275:108kcounts). This low rate could be caused by self-absorption, absorption and the distance to the triggering scintillator or simply by timeout, because the photons do not hit the detector in time.

The setup was similar to fig. 3.16 except that the signals from SiPM9 and SiPM10 were delayed 11ns with the Logic Delay (appendix5.2.6.7) +1ns from the cable.

fig. 3.19 shows the timing. Several peaks indicate reflections, impurities, etc. The width is 6.5 ns which is even wider than 4 ns (3.6.4) respectively 2.3 ns (3.6.3).

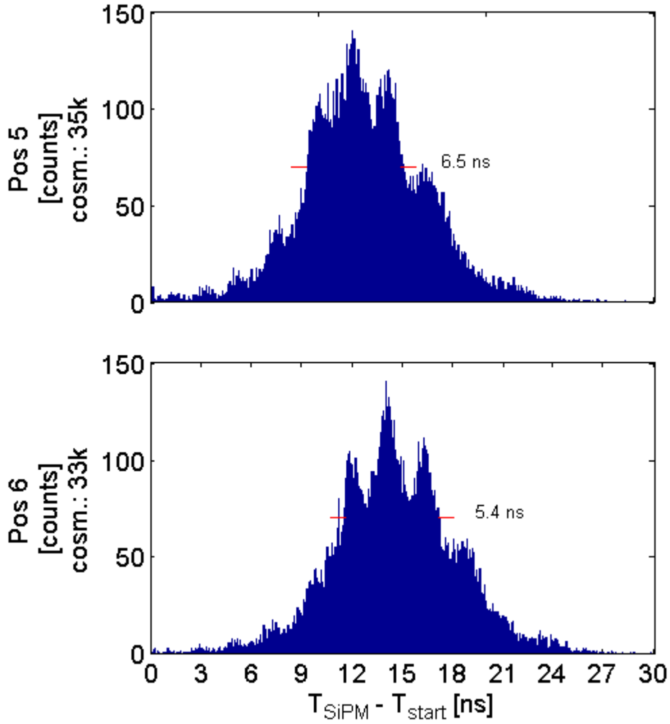

fig.3.19 Timing of the size E scintillator. (4 days)
The timing distribution is becoming broad and structured, due to reflections and impurities.

3.6.6 SizeB scintillator test (half size A)

For simple position detection in the final SIDDHARTA-2 setup another approach could be to split the size A scintillator into two, so a particle hitseither the upper or lower scintillator (see 1.2). I wrapped two prototypes(approximately half of size A:size B, p. 8) as usual. I testedthe timingalternately, using one as trigger and the other as stop signal. (On second turnthe other way round, with smaller duration) To count only coincidental hits, I prepared anAND fold logic (see following fig. 3.20).

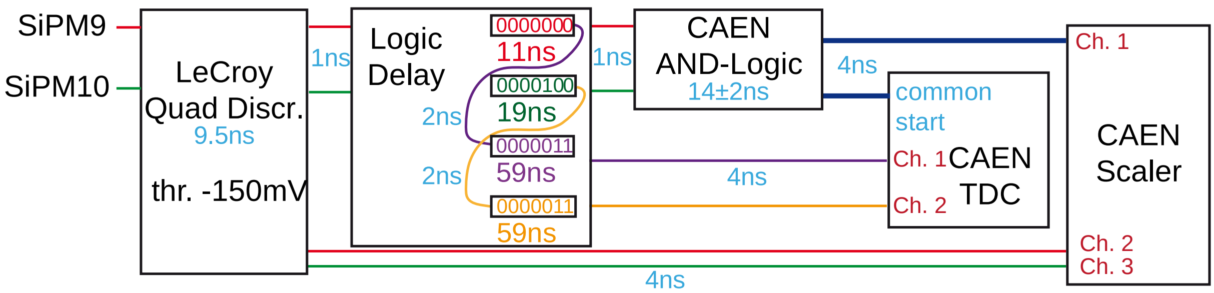

fig.3.20 Setup configuration of the prototype scintillator test.

Naturally the width of the timing (measured with cosmic radiation) is comparatively very small (under 1 ns, see fig. 3.21). While measurements with the source are deformed by many reflections in the small scintillator, cosmic radiation gives a rather sharp peak. (compare3.6.2)

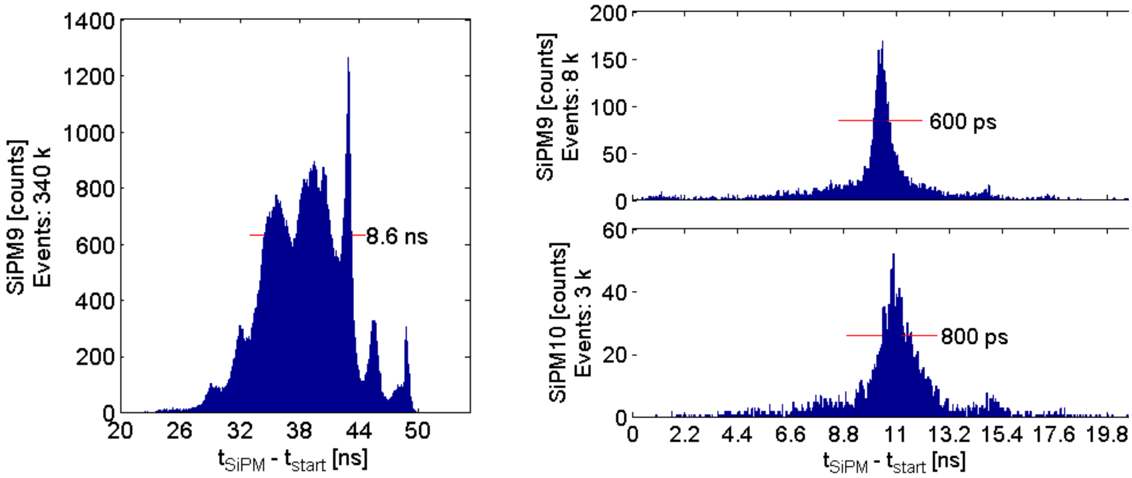

Time differenceusing a Na-22 source. (51min)

Time difference measuringcosmic radiation (SiPM9: 11.5h; SiPM10: 4.3h), each triggered with the other one.

fig.3.21 Timing of sizeB scintillators.

3.6.7 Jitter of scintillation detectors

To measure the rise time differenceof signals(see fig. 3.22 oscilloscope screenshots) created by the SiPM (variation of amplitude)I used an oscilloscope.It provides the ability to statistically acquire this data, using 10% to 90% of the signals amplitude (fig. 3.22,top) to avoid taking distortions into account.It further averaged the data over 4096 events. These measurementsI performed with different scintillatorsizes (see p.8).

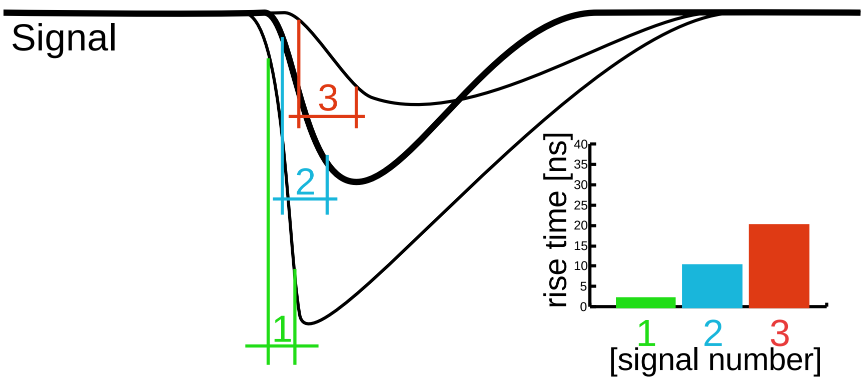

Sketch of the rise time differences between signals; 10% to 90% of the amplitude are used to avoid distortions.

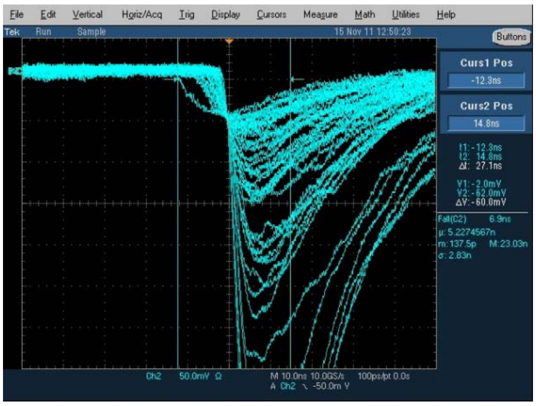

SiPM9 signal from cosmic radiation to studythe risetime

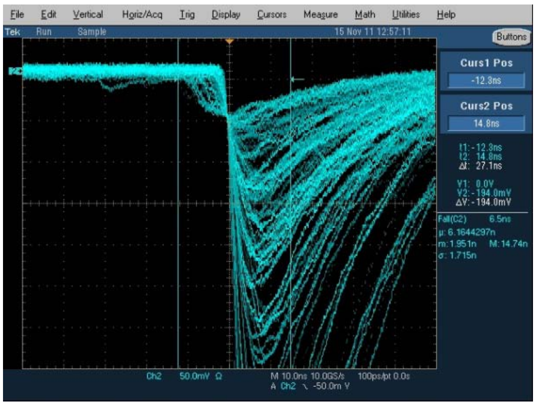

SiPM9 signal of a radioactive Na-22 source

fig.3.22 Rise time differences/jitter measurements.

The results are shown in the tables below.

cosmic radiation	mean[ns]	min [ns]	max [ns]	Sigma
SiPM9 (size B)	5.2	0.1	23	2.8
SiPM10 (size B)	5.9	1.1	17	2.1

The detectors arepositionedon top of each other.

source	mean[ns]	min [ns]	max [ns]	Sigma
SiPM9 (size B)	6.2	2	15	1.7
SiPM10 (size B)	6.1	1.3	15.6	1.7
SiPM6 (size A)	7.4	1.6	29	2.2
SiPM5 (size A)	7.3	1.6	21.9	2.2

3.6.8 Open front end reflection test

We were interested in the question of reflections coming from an open front end face (without mounted SiPMs)of the scintillator. First I measured with the usual wrapping and later removed the Teflon as well as the aluminium from the end face of the Scintillator (size D, p. 8). To provide light tightness Isealed it again only using isolating tape.Setup: U-profile with only SiPM1 mounted for TDC start on top.The following fig. 3.23 shows that the difference is insignificant.

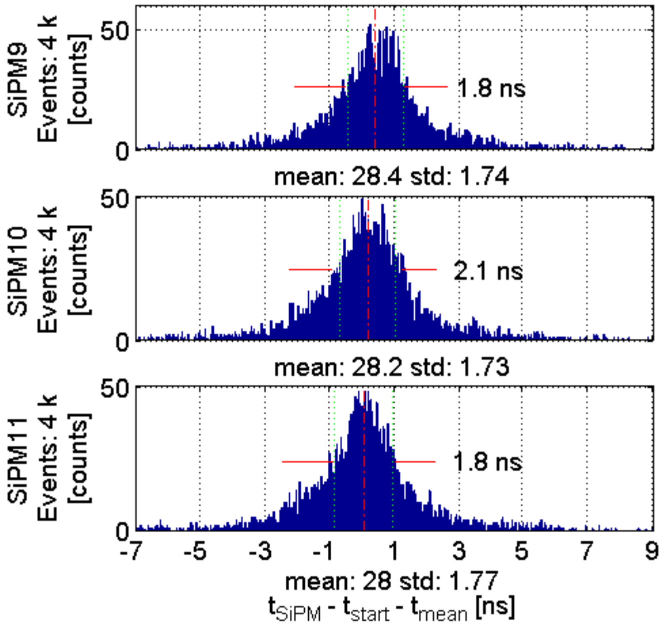

open ending, 4700 events (50h34min)

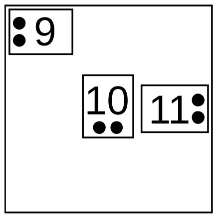

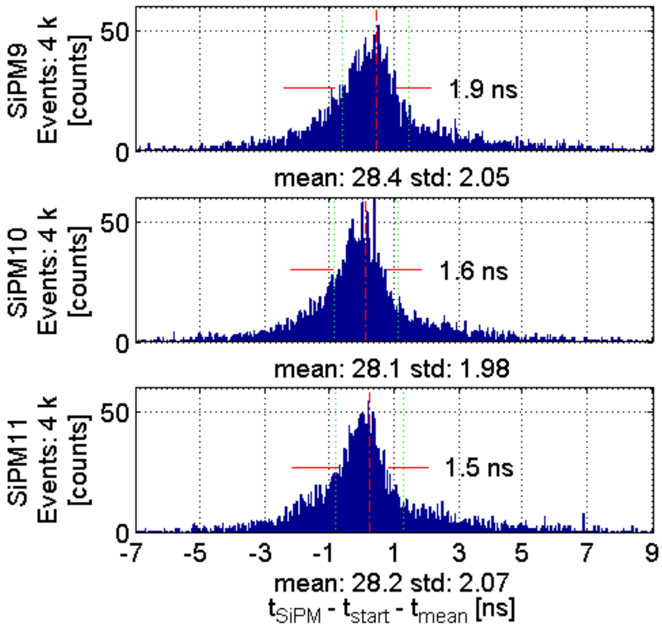

closed ending, 4700 events (44h23min)

fig.3.23 Timing differenceof none/reflectingend face of the scintillator. The rate is normed to 4700 events(cosmic radiation) for comparison.The red line indicates the mean value and thedotted green line the standard deviation.

3.7 PREAMPLIFIER AND INTEGRATED POWER SOURCE

The plan is to use up to 200 detection units in the final SIDDHARTA-2 setup, which leads to the problem of supplying every single SiPM with an individual bias voltage, as well as powering the preamplifiers. Further space is limited, so an on-board bias source is necessary and to save even more space a discriminator could also add some more compactness to the setup.In the following chaptersI additionally discovered how the performance of the SiPM is changingdue to temperature fluctuations.

3.7.1 PREAMPLIFIER LINEARITY

To simulate aSiPM, I used the HP Pulse Generator (see 5.2.10) andin/decreasedthe signal stepwise with anattenuator (see 5.2.6.1).The fact that the SiPM plug is not grounded forced me to use the negative pole of the high voltage connector as mass and the anode connector of the preamplifierto insert the generated pulse. I eliminated reflections (cable) with a potentiometer (~58Ω), which I soldered parallel to the signal.

I chose to generate a saw tooth signal with a frequency around 2.37MHz and I variedthe amplitude between 4mV and 550mV as well as thepreamplifier bias between 5V and 10V. As shown in fig. 3.24 there is a strong noise in response to signals of amplitudes smaller than 15mV. While amplitudeslarger than 100mV saturate the amplification.fig. 3.25 shows the pulse amplitude of the generator compared to the signal at 5V, wherethe preamplifier is linear and thesaturation starting from approximately 150mV.The results are the same for all tested preamplifiers.

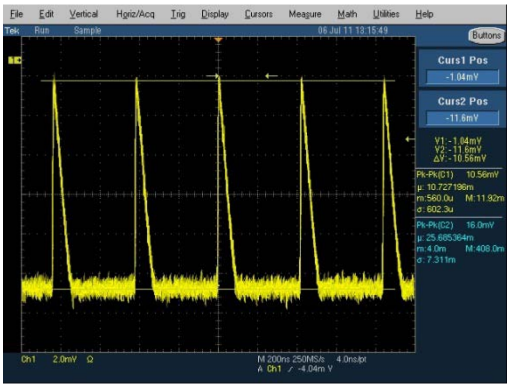

Signal In: 10.5mV (inverted)

Signal Out

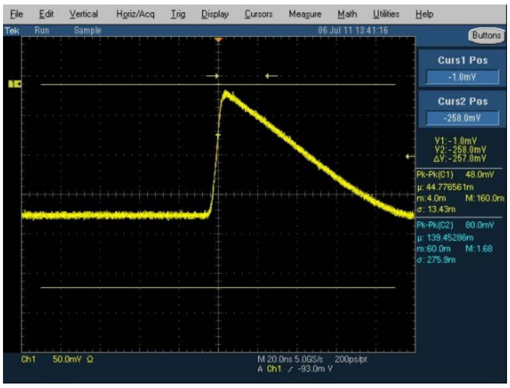

Signal In: 150mV (inverted)

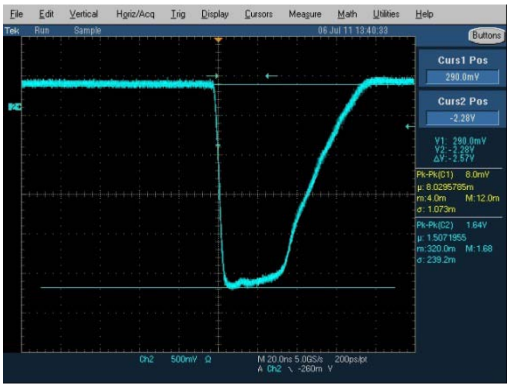

Signal Out, saturated

fig.3.24 Preamplifier signal in/out comparison
Strong noise in response to signals of smaller amplitudes (<=15mV). Signals larger than 100mV saturate the amplification.

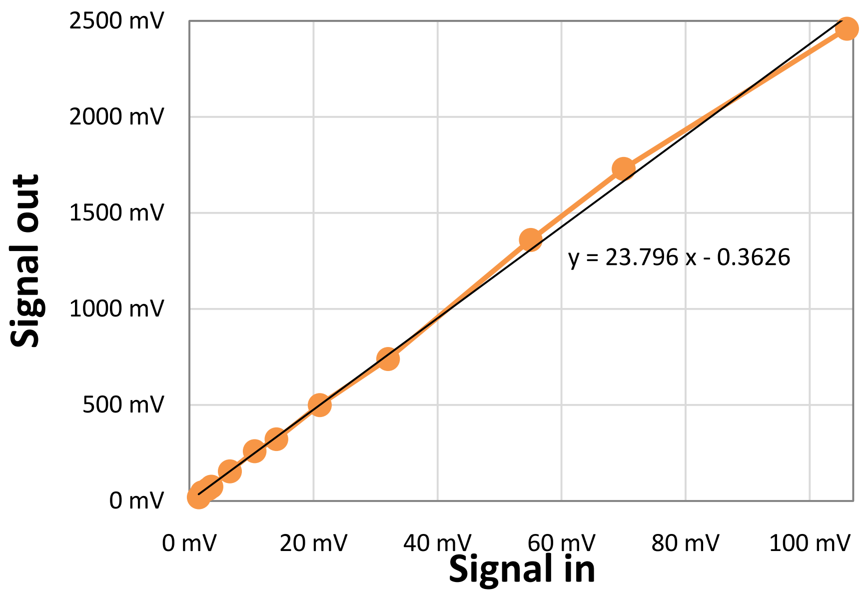

fig.3.25 Preamplifier linearity (5 V power supply).
Generated pulse (signal in) versus signal output shows thatthe linearity is provided for 5V biasvoltage.

3.7.2 CAMAC DEAD TIME TEST

The question of how much dead time the Camac modulesproduce(especially the ADC and the PC connection) is answered in this chapter. I used a NIM counter to acquire the rate of the discriminator and every NIM module. The signalswere provided by one size A (p. 8)scintillator with SiPM3 and SiPM4 mounted.I measuredfor10s and thecountingdifference between a simple ADC setup and the direct countis drastically:

t=10s	[counts]
ADC	6,5k
Counter	237k

To exclude the possibility that any component of theelectronics is slowing down the measurement, I checked the counting rate of every part. (While measuring the fold logic, I connected only one channel.)

t=10s	Gate [counts]	Logic Delay [counts]	Fold Logic (1Ch) [counts]	Fold Logic (AND) [counts]
SiPM4 1st run	283k	280k	277k	177k
SiPM4 2nd run	292k	291k	286k	
SiPM3 1st run	183k	181.5k	180.5k	
SiPM3 2nd run	187.5k	186k	183k	

As can be seen, the signal loss of the NIM modulesis negligible since the measurements werenot taken at the same time and there are many factors influencing the signal. The limiting factor of the ADC readout is the processing speed/dead time of the device.During further measurements, this information loss has to be taken into account. Either the source rate has to be reduced, or a faster ADC should be used.

3.7.3 CURRENT/VOLTAGE SOURCE PERFORMANCE

3.7.3.1 CURRENT VERSUS VOLTAGE SOURCE

fig.3.26 Setup configuration of constant current preamplifier counting.

Some temperature fluctuations can never be ruled out, therefore a regulation mechanism has to be included in the electronics setup. Since controlling the currentis easier to handle and levels temperature fluctuations,the institute's electronic workshop developed adedicated preamplifier with an integrated current source. For temperature stabilization a resistor (linear temperature behaviour) connects the monitor and control pin of the microchip (the current source for SiPM bias voltage). Due to the fact that the SiPM is a diode and therefore has a non-linear temperature dependency, this linear behaviour could be inconsistent.

In this early prototype one can adjust the current with a potentiometer. To make measurements, one has to set the current to a level where the minimum breakdown voltage is exceeded.

It is impossible to measure the current while an experiment is running because the measuring devices interfere strongly with the signal output. As soon as the anode of the SiPM is connected to anything except the preamplifier, the signal is distorted.Another problem while measuring the voltage/current on the powered board is that there is a transistor,which I destroyed several times byaccidentally short circuitingthe anode and cathode. To avoid this, the supply should be shutdown. According to the workshop, this problem will be taken care of in the final layout.

Slight temperature fluctuations, including human heat, influence the setup during working days;therefore setting the current is very difficult. A change in the counting rate can be observed on weekends, when the environmental temperature is more stable (only affected by the weather).

In theory there could be a transient effect within the first 1.5 hours, but due to the strong thermal fluctuations it was not possible to observe it.

First measurements (setup: see fig. 3.26)showed that the counting rate is controlled rather well and the temperature inside the carton box is approximately constant. fig. 3.28compares the voltage and current stabilized preamplifier. At the beginning I placed the voltage control unit inside the box for testing reasons and later took it out. An impact can be seen after the cyan line, which is also influenced by the aeration of the box.

Another observed problem is that the current stabilized preamplifier is noisy under a threshold level of around -100mV. (See fig. 3.27) This noise comes from a grounding problem and is in the area of the frequency of the microchip driver (1MHz). The next layout will take care of this with better grounding. First steps were already tested with this prototype.

The noise frequency is in the range of 1 MHz, originating from the high voltage microchip driver

Shape of the Noise, zoomed in

fig.3.27 Oscilloscope screenshots of the current stabilized preamplifier noise.

To get deeper insight of how temperature affects the setup, the next step would be to independently heat/cool the SiPMand the preamplifier, which I tried to achieve in 3.8.

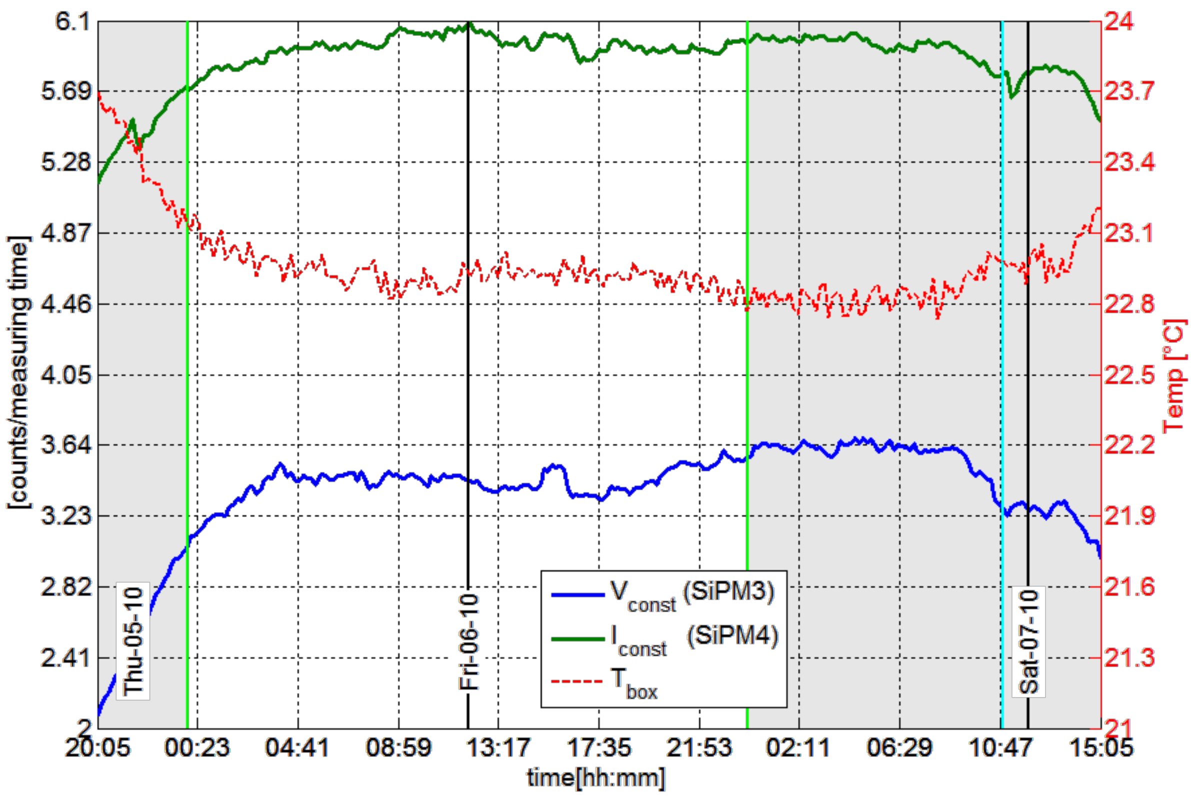

fig.3.28 Comparison of the counting rate of voltage (blue) and current (green) stabilized preamplifiers with a radioactive source placed on the centre of the scintillator.
The counting rate is indirect proportional to the temperature and the current stabilized preamplifier performs slightly more stable than the voltage stabilized (blue).The cyan line at approximately noon Oct. 7th indicates the time, when I took the voltage source out of the carton box. (Aeration; less heat from the source)

It could be misleading to comparecounting rates that diverge too much, because of the fact that voltage and threshold influence the counting rate. (See 3.5 respectively 3.1)

3.7.3.2 Current stabilized versus high standard reference voltage supply

On account of the temperature variation of the surrounding air, I set the air flow of the conditioner to one position (no swivelling) and to 23°C. FurthermoreI increased the current from 1µA to 2µA and replaced the voltage source with the Keithley power supply (appendix,5.2.8), since wewanted a stable reference.I set the voltage to a value that would even the counting rates (70.6V) and increased the threshold to -150mV to make sure the noise of the current preamplifier (fig. 3.27) issuppressed. In addition to the counting rate, LabView logged the monitor output. (appendix, Keithley voltmeter5.2.9) The assembly was the same as in the preceding experiment (3.7.3.1).

The comparison of the results is difficult, since the counting rates vary due to different voltages (See 3.1 and 3.5), but the constant current sourceseems to be more stable. Measurements show thatU_{mon} is varying unnoticeably, so it will be ignored in further experiments. fig. 3.29 shows the measurement over one week (7 days) with no change to the setup. An unsolved incident occurred on 9th of October as both Keithley instruments shut down.

An investigation of the noise (without source) just after the experiment showed a similar result for both amplifiers (usingequal thresholds).

U_{ref}	1330 counts/300s
I_{const}	1200 counts/300s

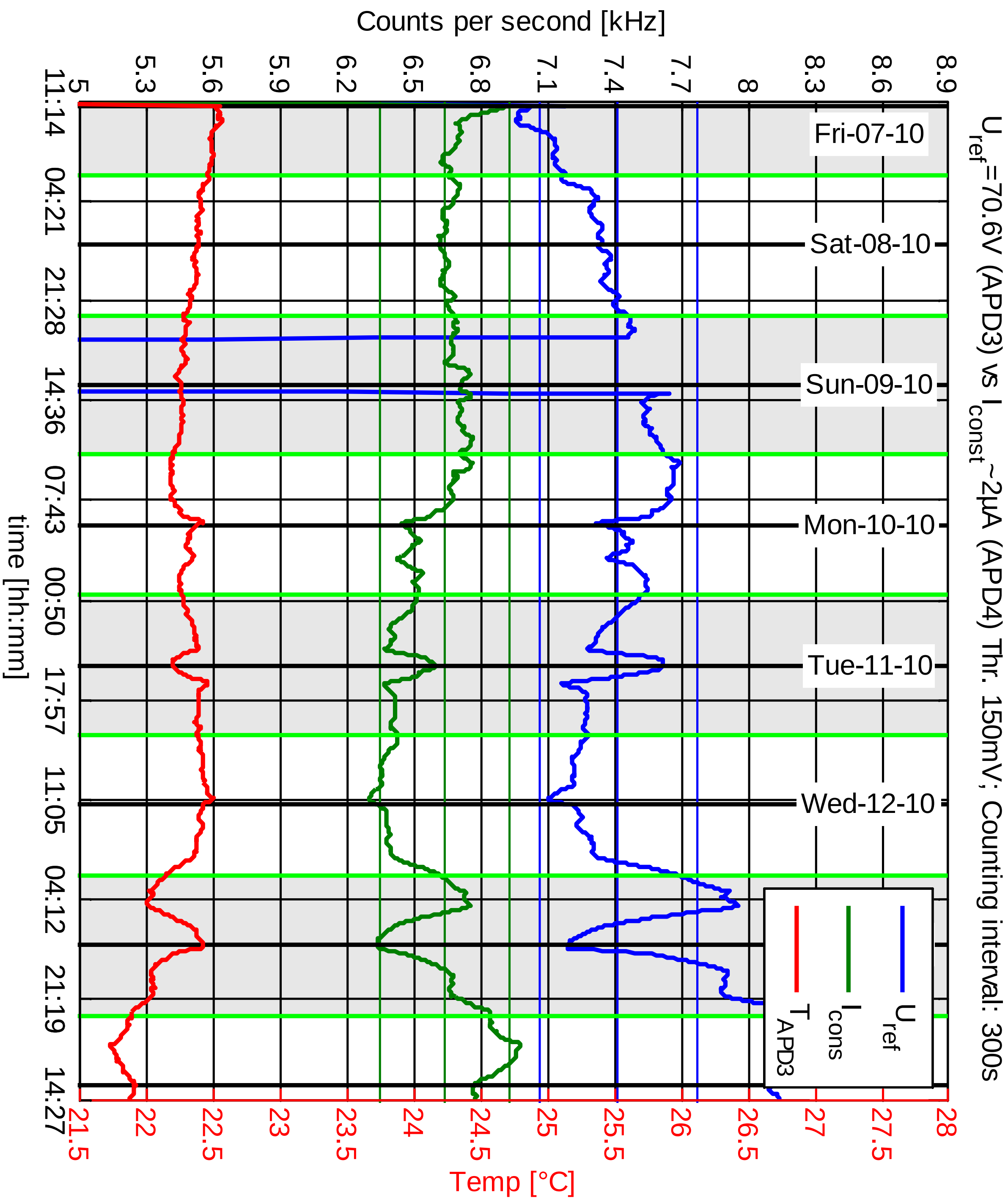

(Keithley and U_{mon}) due to a mains error.

3.7.4 COMPARING NIM ANDON-BOARD DISCRIMINATOR

Either 100 or 200 scintillators will surround the SIDDHARTA-2 setup (depending on the decision of the position detection method; see 3.6.6) so only little space is provided. Therefore we wanted tokeepelectronics placed outsidethe experiment at a minimum and started to develop, respectively test a dedicated on-board device.To check if on-board triggering provides acceptable results, I connected a standalone prototype discriminator (simple discriminator; appendix, 5.2.1.4) located on anadditional board to the signal port of the standard preamplifier (appendix, 5.2.1.1). To use the same SiPM signal, the NIM system discriminateda looped-through signal of this unit. Since this early test boards output of the discriminator is using TTL-logic, which is not accepted by NIM, I had to convertit via level converter (appendix, 5.2.6.11). Furthermore the signal output is differential, which implies that only half of the amplitude can be used. Therefore thesignalamplitude isonly about 2/5thof the original one (see fig. 3.31). To work with it anyways, I used a very low threshold within the NIM discriminator (threshold around -45mV) and adjusted the on-board threshold to result in a very similar counting rate (6k/s; this resulted in a threshold of around-200mV). fig. 3.32 shows that the discriminators respond in the same way and it is possible to use the built-in device.

To supress aDC offset that is altering the signal, Ihad to soldera capacity as shown in fig. 3.30.

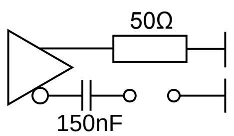

fig.3.30 Capacity soldering for the differential signal.
A capacitor soldered in series, filters the signal offset of the preamplifier.

Amplitude of the loop-through signal

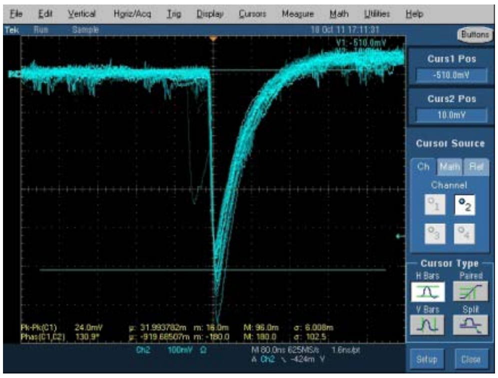

Amplitude of the direct signal

fig.3.31 Comparison of the loop-through and the direct signal.
The amplitudes maximum is only 2/5th of the direct signal.

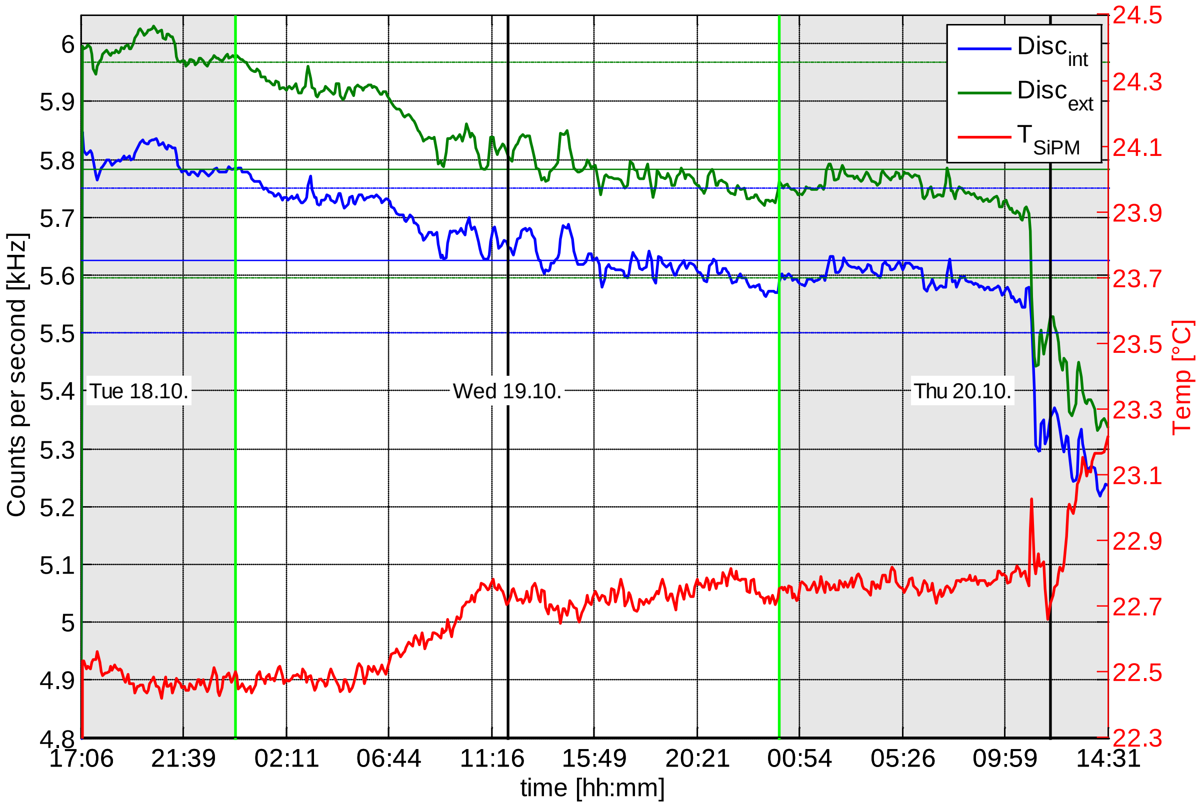

fig.3.32 Comparison between the on-board and the NIM discriminator counting rates.
Both discriminators react in the same way and therefore the on-board device is approved for the final setup. (blue: counting rate integrated discriminator; green: NIM discriminator; red: temperature)

Comparing the results of this test, one can see that the discriminators are almost identical. The additionally logged threshold level is also stable (and therefore not shown).

3.7.5 Improved current system

Since the effect of the thermal stabilization of the on-board current source (see 5.2.1.3) couldnot be improved with the help of a non-linear element (diode), further optimizations had to be made (e.g. optimizing themicrochip control voltage).These include the possibility to (without load) set the desired SiPM voltage and afterwards (with connected SiPM) the current,each with a potentiometer. Since voltage and current are connected through Kirchhoff's law, the settings affect each other. To compare the modified preamplifierwith another temperature dependent system, I used the voltage stabilized source. (See 5.2.1.2)

I connected SiPM5 (~2µA, 71.19V) to the current stabilized system and SiPM7 (71.47V) to the voltage stabilized source.The latter I set to a voltage where the counting rateswere approximately the same.

The setup is the same as shown in fig. 3.26 with a threshold of -150mV and a gate-width of 20ns. The temperaturesensors measured near the digital potentiometer and above the preamplifiers. The produced heat of the digital potentiometer (voltage stabilized preamplifier) seems to raise the temperature to a ~1.4°C temperature difference.

With the counting rates very close together, the current stabilized amplifier shows a more stable performance. (See fig. 3.33) This time also the monitor of the voltage source was logged, which gives the current, using the following formula(4): (2.475V was guessed to be the zero current)

$$I_{APD7} = \frac{U_{mon} - 2.475V}{20mV}\ [\mu A] \tag{4}$$

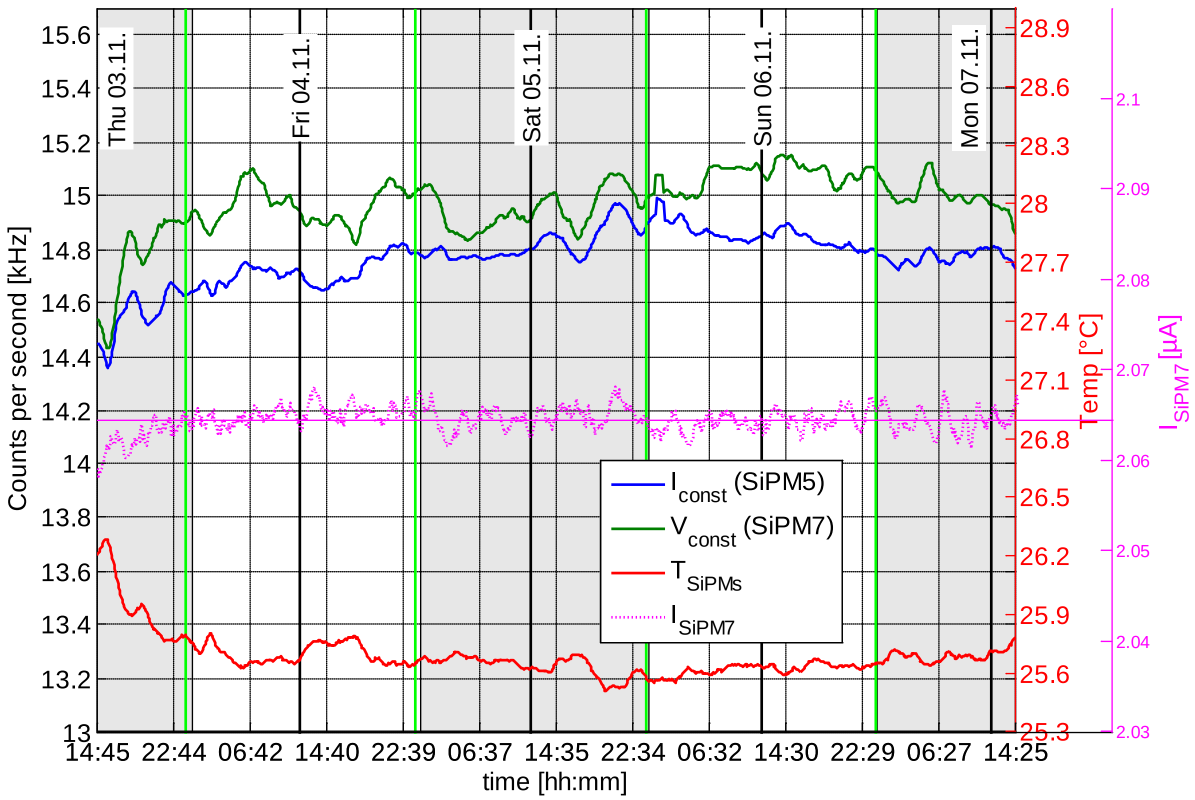

fig.3.33 Counting rate comparison of the modified current stabilized and the voltage stabilized preamplifier. (Acquiring over 4 days)
The counting rate fluctuations of the current stabilized preamplifier(blue) are smaller than the ones of the voltage stabilized (green).The pink signal indicates the current taken from the voltage stabilized monitor port.

3.8 SiPM temperature dependence

As can be seen in various tests, the counting rate and QADC spectrum is altered at different temperatures. This happens due to the fact that the counting rate is increasing or decreasing depending on the SiPMs temperature (current). To antagonise this process the measurement should take place in a sealed, evacuated and grounded box (see fig. 3.35 and chapter 2.5) with the possibility to separately cool the preamplifier and SiPM.

3.8.1 Standard preamplifier cooled

First I cooled down only the SiPM to around -10°C (temperature at the Peltier Element: -35°C)but not the preamplifier.The bias voltage was provided by an external source (Keithley, appendix5.2.8) and not on-board, so cooling was not necessary.Since the bias voltage was held constant, the current increased, raising the counting rate drastically with decreasing temperature (see fig. 3.34). This was the reason why the ADC denied measuring after some minutes (dead time problems). I corrected the bias voltage to 69.5V (from 71.19 V, see SiPM 6:appendix 5.2.1) to lower the rate. The setup was kept rather simple and I just split the signal and connected 80% to the discriminator and 20% to the ADC, this attenuation has to be kept in mind when setting the threshold.

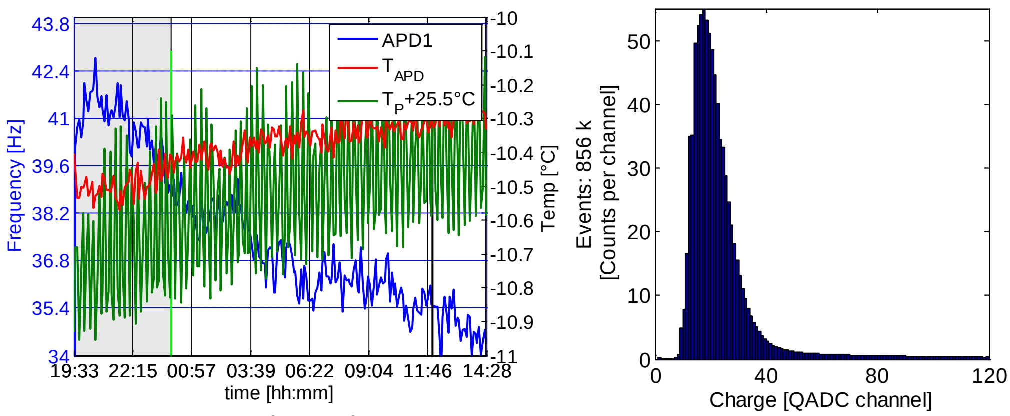

temperature and counting rate.

fig.3.34 QDC spectrum and temperature measurement withan uncooled preamplifier. (Cosmic radiation)
The temperature graph is unclear and just added to give an idea of the fluctuations and a temperature drift (in the (blue) counting rate) that has to be investigated further. (Measuring time 7h)

Until now I powered the Peltier element just with a constant current to test if the inertness due to the aluminium plate and the copper cable (acting as buffer) is sufficient cancelling out the oscillations of the water cooling. The general drift in the system seems peculiar, since the water cooling should keep the temperature.

The first solution for stabilizing the oscillations was to just cool the preamplifier and therefore cut the influence from the environment, which is done in the next experiment. The difference is shown in fig. 3.36.

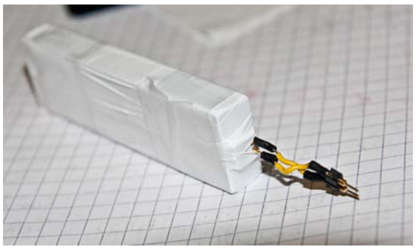

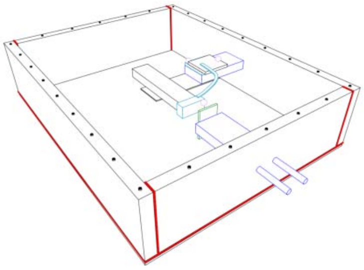

Extension of the SiPM pins

fig.3.35 Box and scintillator for temperature stabilization box
For more flexibility the pins were extended with cables and a connector (adding around 1cm of reach).Due to rubber gaps (right picture; red lines) between the parts, the box acts like an antenna,see 2.5 for more detailed graphics and information.

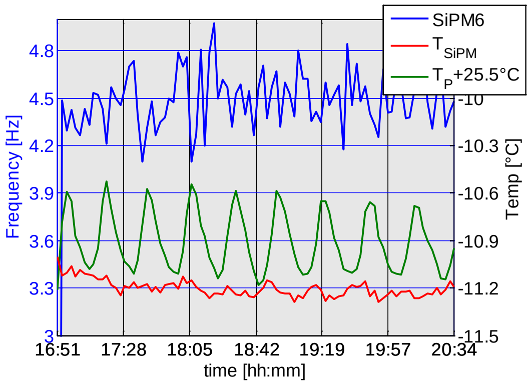

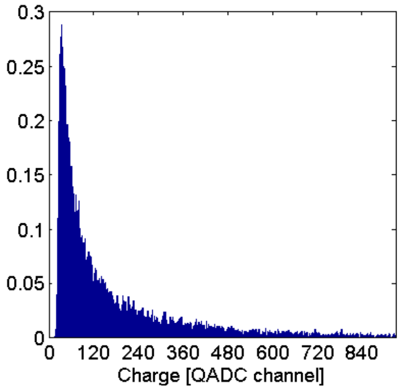

Temperature and counting rate.

Charge ADC spectrum

fig.3.36 Counting rate (cosmic radiation), temperature and QADC spectrum of acooled SiPMand a cooled preamplifier
The system seems more stable (3.75h measuring time) and the drift is gone. It is possible that the second cooling helps to lower the temperature of the box itself and therefore the environment is ignored more effectively.

3.8.2 Improved current stabilized preamplifier

Since a slightly improved version of the current stabilized preamplifier was ready, the test with the standard preamplifier stopped. As I showed in 3.7.5 the improved version of the current stabilized preamplifier works well in the laboratory. After putting it into the box, I measured very high interferences coming from Wi-Fi and also the already damped 1 MHz signal resonates in the box to an even higher amplitude.

To fix this we replaced every cable and remounted everything. The electronic engineer improved the grounding of the preamplifier, which led to a lower but still very high noise. Neither tiling the box with aluminium foil, nor surrounding and grounding it,improved this problem. The gluing gaps between the box’ walls (filled with more or less isolating glue),rubber sealing at the top, etc. make these problems worse.

The only solution is to build a new box with conductive connections between all parts.

4 OUTLOOK AND CONCLUSION

Within this thesis the results of certain preamplifier tests are discussed. There are three different possibilities for the final setup and the preamplifier with thermal-stabilized current source convinced with a combination of stability, usability (setting the current is more easy) and compactness.

Of further interest was the performance of different shapes and sizes of the scintillators. It is not yet decided if the final SIDDHARTA-2 setup will consist of 2 rows of small (100mm long) or large (200mm long) scintillators. Since 2 rows could only give a binary localisation, while one long detectorcould give more precise results (at the cost of more equipment (TDC,…)).

For good active shielding a reliableSiPM signal is necessary. The performance on different front end face positions was suitable and the timing adequate. Furthermore the tests showed that the used SiPMs are strongly correlated to temperature fluctuations therefore not only a current stabilization but also a temperature regulation should be provided. Of course the cooling of the whole SIDDHARTA-2 experiment should provide a temperature at stable conditions.

The final active shielding will consist of a scintillator ring of about 100 (size A) or 200 (size B, p. 8) detector units around the target cell and the SDDs. Therefore the detector units should be simple, vacuum compatible and compact. Our concept fulfils these requirements.

Further development and testing should be done, regarding following topics:

- The temperature stabilization of the new preamplifierfor the SiPM has to be confirmed.
- The long term stability and reliability has to be tested.
- Definitions of optimal bias voltage/current ratio have to be found.
- Possibility of an on board TDC has to be checked, developed and tested.

Following requirements are necessary for final detection unit:

- One has to find an easy to apply and reproducible scintillatorwrapping. (e.g. Tape, sprayed or glued)
- A durable, reliable, simple and robustSiPM- and preamplifier-mounting has to be found.
- Thedistortions of the preamplifier have to be further minimized.
- Altogether the setup should provide maximum measurement area at minimum space consumption.

Acknowledgements

15 Semesters are a long time, where you meet many interesting people. My work in the Fachschaft Physik (ÖH – students union UT Vienna) took a great deal of my time at the university. Several events, seminars, workshops and nice conversations after exhausting lectures, labs,… made it a great period in my life. Therefore I want to thank everyone I met, who made life easier and better, as well as the ÖH UT Vienna for doing such a great job and the staff (profs, etc.), where I found some friends too.

For many summers, where I acquired scientific work experience and finally worked on my diploma thesis, I want to thank the Stefan Meyer Institute and all its staff members as well asits students for giving me such a 'like home' feeling. Especially I want to thank Johann Martonand Johann Zmeskal for this interesting work, their support and the advisory; Herbert Schneider for not only supporting me, but also giving me some insight into the secrets of electronics and giving me some practical advice. Further Martin Diermaier for being my (diploma thesis) partner in misery, lunch mate, scientific discussion buddy,… I want to thank Tomoichi Ishiwatari and Ken Suzuki for their ideas, explanations and scientific input; Leopold Stohwasser and Doris Stückler for their patience with technical support and all the others, which are not mentioned and but not forgotten!

Last but not least I want to thank my family for providing everything I needed in this life period, for every support, for motivating me, for the opportunities,…

5 Appendix

5.1 Programming

For data acquisition I drew a program in LabView and improved it stepwise. MatLab was the tool for data analysis and illustration. With every test setup and measurement, the programs were improving and developing. The flow and usability enhanced and the LabView schematics got more readable. In this chapter I introduce the main methods for data acquisition and processing.

5.1.1 MatLab

I chose MatLab for data analysis because it can handle large amounts of data and its plots are highly customizable. Like every programming language MatLab has its advantages and disadvantages, further there are some very useful features, I would like to present. I use the student license of MatLab R2009a.

5.1.1.1 Tips: cell mode and word-wrap

One of the features of the programming environment I used mostis the cell mode. MatLab gives the possibility of splitting a program into several parts and run them independently. A cell starts with `%%` which is similar to a comment`%`, so one can name the cells in a semantic way. For instance:

```
%% ++++++++ Initialisation +++++++++
```

These cells can be executed with pressing `CTRL+Return`.

Sometimes a command has so many parameters that it is more readable when wrapped into several lines. This can be achieved by closing a line with three dots`...` and precede the code in the next line.

```
Command(Parameter1, ...
Parameter2);
```

If you want to output some info on the screen without showing ‘`ans =`‘ and a new line, you can use following command:

```
disp('Infotext')
```

5.1.1.2 File read-out

MatLab needsa working directory, where it looks for files and programs. If you want to make a flexible program, it is a good idea to put a ‘change directory’ (*cd*) at the beginning of the program. Sometimes it is also a good idea to clear the variables memory, to make sure the running program has enough resources.

My data consisted of tab separated columns and I read them out using following code:

```
clear;
cd 'HDD:\Folder';
Num=1;
fid = fopen('Data');
DataVariable= textscan(fid, [repmat('%f ',1,Num) '%s'], ...
'Delimiter', '\t');
fclose(fid);
```

`Num` is a variable I chose for the number of columns that is passed to the `repmat()` command. `Repmat()` copies the pointer in the format string `Num` times. I had to set the delimiter parameter, because the last column consisted of a date string, which is otherwise misread. It is important to `fclose` the file; otherwise the file identifier variable (`fid`) runs out of range after a while.

If there was too many lines of data (I read the file in chunks, see the `textscan`command help) or I wanted to load several files, I attached the data one by one to a variable in the following form:

```
forx=1:length(DataVariable)
   Data(1,x) ={ [Data {1,x} DataVariable {1,x}]};
end
```

Since my last column was a date string, I exchanged it with a floating point number, to convert the data to a matrix (which is simpler to use than a cell structure). To make sure the data is sequential, I sorted it afterwards.

```
Data {Num+5}=datenum(Data {scal+5});
Data =cell2mat(Data);
Data =sortrows(Data,scal+5);
```

5.1.1.3 Plotting graphs

To not accidentally override a figure of a different cell, I defined a figure for every purpose. The clear figure (`clf`) command should delete all content of a figure, but sometimes one has to close the figures window to make sure everything is refreshed.

```
figure(3)
clf
```

Every focused figure can be addressed with the Current figure handle (`gcf`). With this handle one can for instance define a position on the screen and the size of the window:

```
pos=[x y width height]
set(gcf, 'position', pos);
```

In this case the position data is in units of pixel.

Plotting a standard x-y plot is accomplished using the`plot()` command. If it is necessary to get a second y axis, `plotyy()` is an easy to use command. For more axes one has to use workarounds or rather complicated tricks. A good point to mention here is the KISS[4] principle.

[4] http://en.wikipedia.org/wiki/KISS_principle

Concerning figures: more and easy to understand figures are better than one overloaded.

To plot several graphs in one figure, `'holdon'` makes sure that the next plot command creates a new layer and does not overwrite the old graph.

```
21 [AX,H1,H2]=plotyy(X1, Y1, X2, Y2);
22 hold on;
23 line(X3, Y3,'color','g','LineWidth',2);
```

5.1.1.4 MODIFYING FIGURES

The automatically generated axis limits can be adjusted with the simple command:

```
24 xlim([xmin xmax]); %exchange “x” with “y” for y-axis
```

To get access to further properties one can use the current axes handle (`gca`) in combination with a `set()` command. (see line 28, with `gca` instead of `AX(x)`)

If the figure has more than one axis they have to be addressed separately, to find them one can use the `findall` command connected to the current figure (`gcf`).

```
25 AX = findall(gcf,'type','axes');
```

With this axis handle it is possible to access the properties and for instance set the limits, ticks, ticklabels, etc. To quickly access the subdivisions of the axes, I recommend setting a variable like `subD` (see line 27) and round it to an appropriate accuracy.


```
26 maxmin=[min max];
27 max2min=maxmin(1):round((maxmin(2)-...
   maxmin(1))/subD*100)/100:maxmin(2);
28 set(AX,'position',pos)
29 set(AX(1),'YLim',maxmin)
30 set(AX(1),'YTick',max2min)
31 set(get(AX(1),'Ylabel'),'String', 'T_{SiPM} [°C]')
32 xlabel(AX(2),'Time [hh:ss]');
```

To subscript more than one letter, one has to use brackets after an underline. (`T_{SiPM}` results in T_{SiPM})

Handles to objects (`line`, `bar`,…) are required to address the graphics' properties (`colour`, `line`,`width`,…). With them one can select the plots displayed in the legend (see line 34) or change the order of the graphs (see line 35).

```
33 H = findobj(gca,'Type','line');
34 legend([H(1) H(1)],'T_P','T_{SiPM}','Location','NW');
35 set(gca, 'Children', [H(2) H(1)])
```

5.1.1.5 Common problems

- Avoid variables named like functions; like: *max()*, *min()*, *limit()*,...
- Wrong working directory can lead to errors
- Numerical file readout requires point for decimal numbers
- Numerical variables should be converted to a string, when including them in Labels, etc.: use *num2str(var)* to convert.

5.1.2 LabView 2010

5.1.2.1 Communication with the Camac System

There is no documentation on how to use the SubVIs provided by Wiener butsome rather complex examples can be found. As soon as the different functions are clear, it is obvious that just bunch of VIs are needed to achieve the desired results.

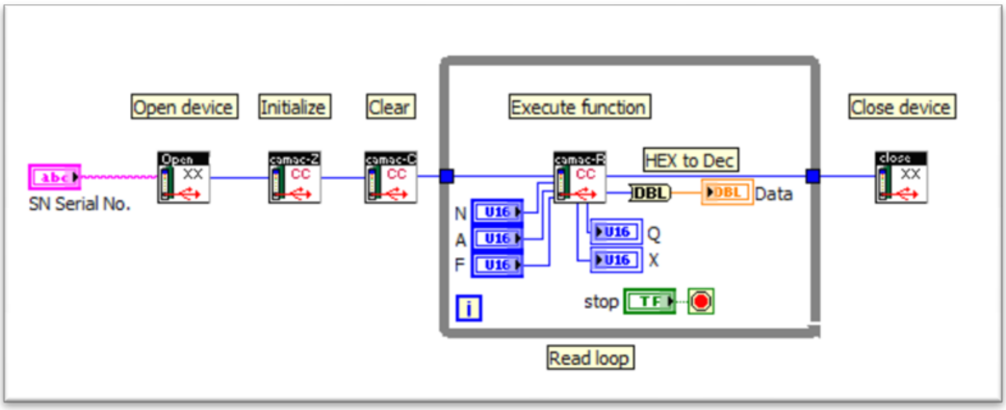

fig.5.1 LabView program for data acquisition with Wiener Camac system. Left of the loop the initialization part is located;it demands the serial number, which can be read out with the Wiener tool. (Or found at the rear of the module)In the loop the read function can be found. N is the Camac slot of the card to read out. A is the address of channel. F is the command to be executed (read, clear, etc.). Q = 1 if there was an event (LAM). X =1 if command is accepted.

First the device has to be initializedwithits unique serial number, this returns a handle. With this handle all other VIs are communicating with the Camac System. (Every VI has a handle in and out channel) The read function is a very versatile one, it allows checking the LAM status to use it for conditional cases, to read out data (provided in hexadecimals), to clear the module, enabling/disabling LAM, etc. This only depends on which functions are provided by the particular Camac module (see 5.2.5)

There is another but inconvenient method to send commands in hexadecimal format, but this would be only interesting when using the command stack (see 5.2.5).

5.1.2.2 Multi-readout SubVI

To read out more than one channel it is necessary to send multiple read commands. Due to the fact that the provided Camac USB communication interface is somehow not able to use its speciality (the command stack) one has to send every command separately. To achieve this faster, an array filled with the signal (channel) addresses is handed over to a SubVi (fig. 5.2) that reads out the module and has connectors for every essential in- and output.

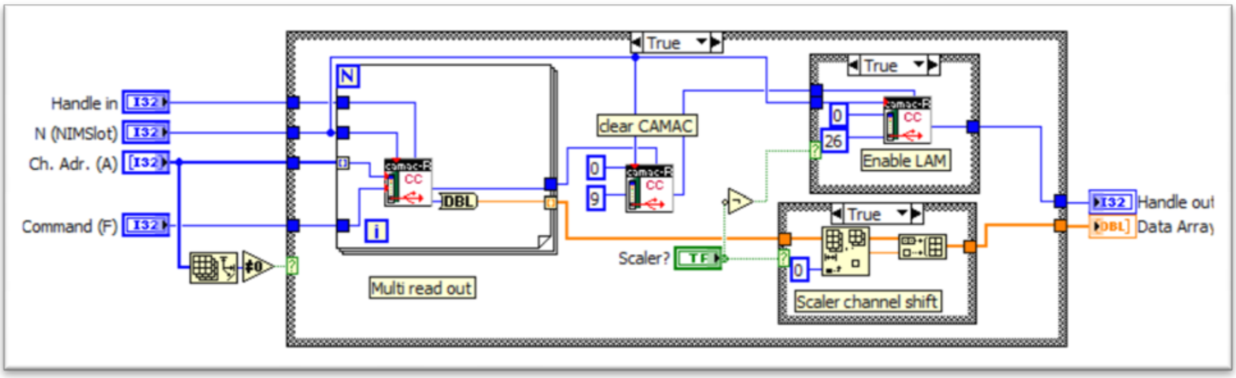

fig.5.2 SubVI for multiple channel addressing.
A is an array that contains the channels to read out. The data is automatically converted from HEX to DBL and "Scaler?" if true, moves the first element of the data to the last position in the Data array (because the data is somehow shifted).

5.1.2.3 File creation and handling

To make sure no data is overwritten, I used the while loop counter as appendix to the filename. The benefit of this is that usually the number is continuous and can therefore easily be used when read out (fig. 5.3).

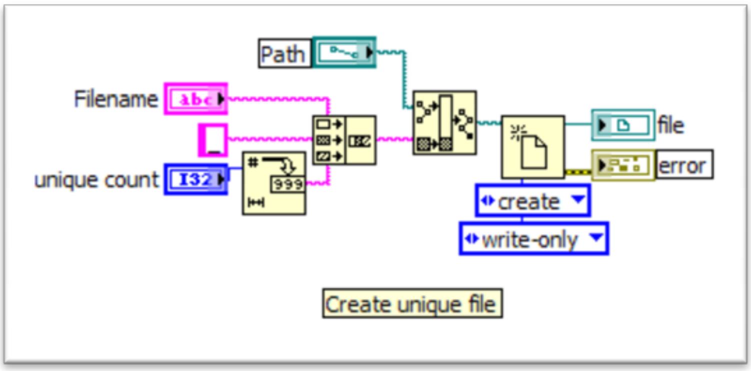

fig.5.3 Createa unique file(filename)
In addition to the custom filename, a unique count (e.g.from the while loop) is attached to the namestring.

A timestamp in the data is also a good idea as well as formatting floating point numbers with a decimal point (fig. 5.4). In my program, when not reading out a specific slot, a tab-stop is applied even if there is no data. To avoid readout problems (and some manual work), double tabs are deleted.

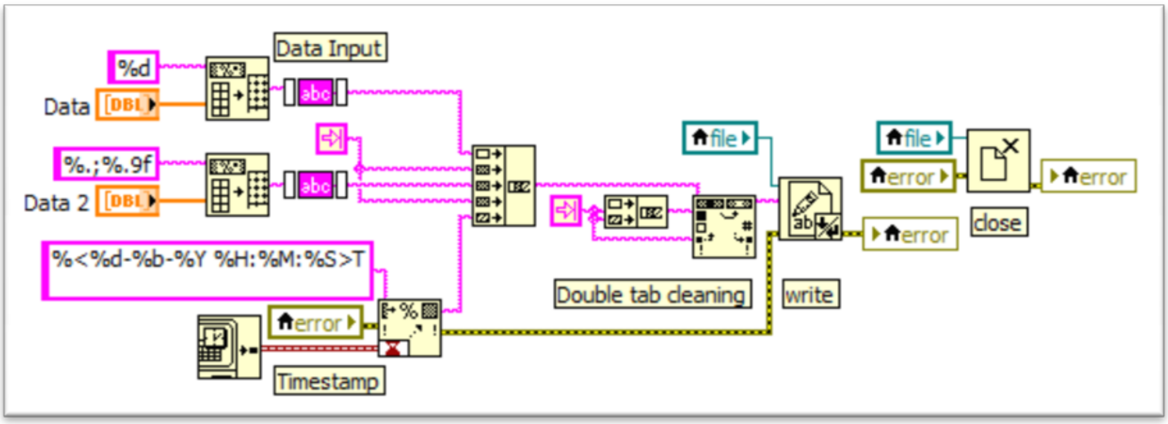

fig.5.4 Write data to file
Data formatting ('%.;' for decimal point) and timestamp (formatted for MatLab datestring read out) are written to the file. Prior to this, double tab-stops are eliminated, to avoid additional work due to read out errors in MatLab. After writing, the file is closed.

5.1.2.4 National Instruments DAQ USB

This chapter and the following figures (fig. 5.5 and fig. 5.6) show how to acquire temperature (voltage) data with DAQmx.

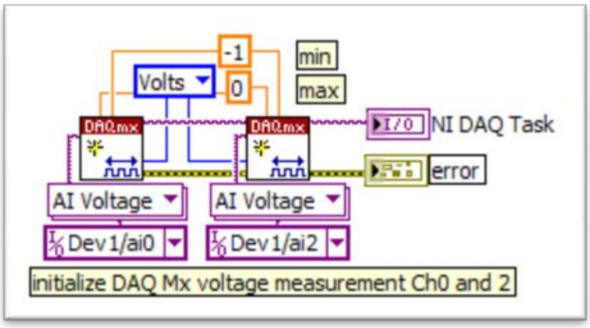

fig.5.5 Initialisation of NI DAQ USB
The read out took place in a while loop.

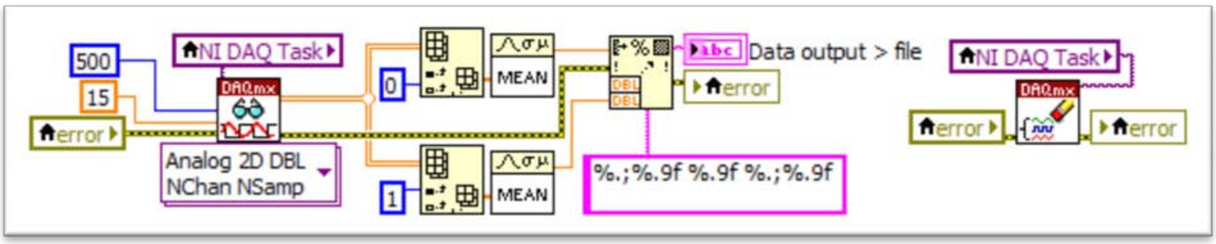

fig.5.6 NI DAQ USB read out. (To put into a loop)
500 samples with 15Hz are acquired and averaged afterwards. The mean values are formatted (decimal point) and put into a string for file output. After this the task is closed (outside a while loop).

5.2 Devices and components

Here I give an overview of the used devices and parts. Exact product names, information, etc. are listed if necessary.

5.2.1 Preamplifiers

Make sure that connector fits thin SiPM wires!

5.2.1.1 Standard preamplifier

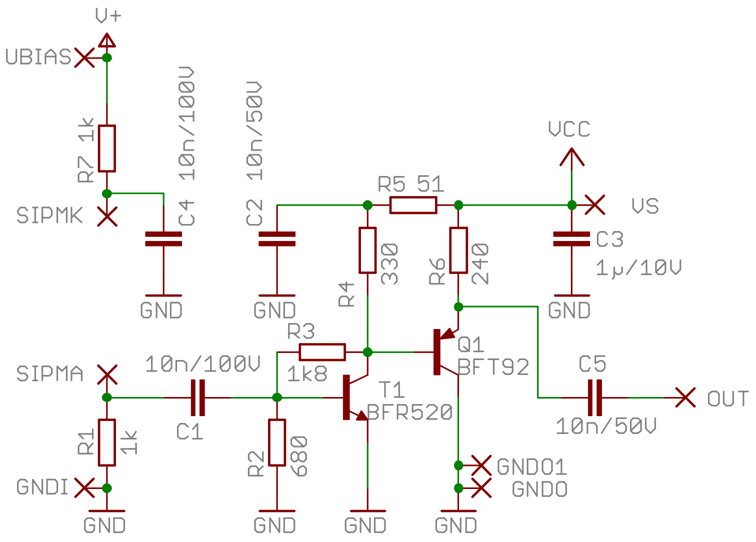

fig.5.7 Circuit diagram of the Hamamatsu standard amplifier.

This is the recommended preamplifier from Hamamatsu; it is set up on an 8x35mm board with connectors for:

- Signal out
- SiPM Bias (around 70V, see 5.2.1)
- Preamplifier supply voltage (5V)
- Plug for SiPM mounting

Since every SiPM (usually) has slightly different characteristics, the required bias differs, so one should provide a power source for each diode. Since the final veto-counter (active shielding) should consist of various SiPMs, there has to be a small and reliable supply unit for each. (See following chapters.)

5.2.1.2 Preamplifier with voltage source

This configuration uses the preamplifier mentioned in 5.2.1.1 but it is supplied by a supply unit, which only requires 8V power supply and generates the high bias for the SiPM which can be set (at least in this early version) with dip-switches. It also loops through the preamplifier supply.

It uses a temperature dependant digital potentiometer, which makes it difficult to set the same voltage at different temperatures. (+0.02V just by human heat) Further the step size could be too big.

5.2.1.3 Preamplifier with current source

A new all in one board was developed by the institute's electronics engineer;it consists of the recommended preamplifier (see 5.2.1.1) as well as a current regulated voltage source. Since the SiPMs power consumption differs with temperature, the voltage is adjusted to keep the current at a defined level.

In this early state the level is adjusted through a potentiometer. Even human heat influences the regulation cycle and there is also a decay time, which makes it nearly impossible to set the current at non-regulated climate conditions.

Accidentalconnection of anode and cathode, when the preamplifier is powered may result in the destruction of a transistor at the cathode area. In case of such an event it has to be replaced. Therefore it is important to switch off the power supply every time when preparing to measure U_{SiPM} or I_{SiPM}. In this early prototype the microchip generates a noise due to insufficient grounding. Applying a grounded copper plate on the backside of the preamplifier improves the signal. These problems will be taken care of in the next layout.

5.2.1.4 Preamplifier with discriminator

The discriminator has a conversion delay of 7ns.

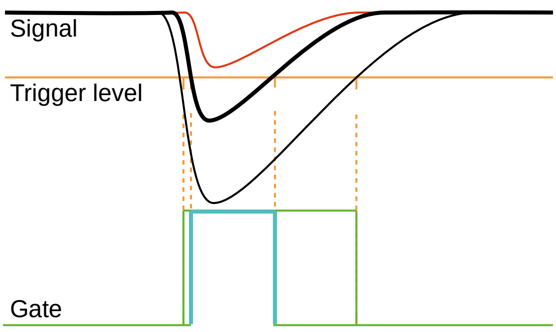

fig.5.8 Schematics of the operating mode of a simple discriminator.
On a fixed trigger level the gate is opened on the negative slope and closed on the positive. Due to this fact gate size varies with signal width/height.

5.2.2 SiPMs

The SiPMs are manufactured by Hamamatsu[5].100µm pixel size:

SiPM 1:	Type: S 10362-33-100C V_{op}: 70.76 V	Serial No.: 1C000532 Dark: 9.5M (0.5 thr)
SiPM 2:	Type: S 10362-33-100C V_{op}: 70.87 V	Serial No.: 0D000520 Dark: 9.4M (0.5 thr)
SiPM 3:	Type: S 10362-33-100C V_{op}: 70.93 V	Serial No.: 0D000519 Dark: 9.7M (0.5 thr)
SiPM 4:	Type: S 10362-33-100C V_{op}: 70.94 V	Serial No.: 0D000518 Dark: 9.9M (0.5 thr)

50µm pixel size:

SiPM 5:	Type: S 10362-33-050C V_{op}: 71.19 V	Serial No.: 0J002819 Dark: 5.8M (0.5 thr)
SiPM 6:	Type: S 10362-33-050C V_{op}: 71.19 V	Serial No.: 0J002824 Dark: 6.4M (0.5 thr)
SiPM 7:	Type: S 10362-33-050C V_{op}: 71.19 V	Serial No.: 0J002823 Dark: 6.1M (0.5 thr)
SiPM 8:	Type: S 10362-33-050C V_{op}: 71.17 V	Serial No.: 0J002818 Dark: 5.9M (0.5 thr)
SiPM 9:	Type: S 10362-33-050C V_{op}: 71.16 V	Serial No.: 0J002816 Dark: 6M (0.5 thr)
SiPM 10:	Type: S 10362-33-050C V_{op}: 71.14 V	Serial No.: 0J002817 Dark: 6M (0.5 thr)

The given (datasheet) values are at 25°C.

5.2.3 Optical grease

Saint Gobain BC-630 Silicone Optical Grease[6]

5 http://www.hamamatsu.com
6 www.detectors.saint-gobain.com/Detector-Assembly-Materials.aspx

5.2.4 SCINTILLATORS

I used Bicron premium plastic scintillators

Handling instructions:

- Keep factory applied protection foil as long as possible (avoid wetting)
- Wear clean soft cotton gloves. If not possible, wash hands.
- Protect material from most organic solvents and vapours
- Clean scintillator with: clean water, soapy water followed by a clean rinse
- Drying with oil-free compressed air or gently patted dry with clean, soft non-abrasive cloths or paper towels

Sanding
Remove turning lines at 90° angles with 240, 400 and 600 grit silicon carbide waterproof paper (using water).

5.2.5 CAMAC SYSTEM

5.2.5.1 WIENER CC_USB

To work with the device in LabView, one has to find out the serial number via XXUSBWin tool (or from the rear side of the hardware), which can be downloaded from the manufacturers website together with the LabView SubVIs.

5.2.5.2 LECROY 2249W 12CH ADC

- QDC (charge measuring)
- 1980 Counts = 11bit
- opening and closing times: 5 ns (time to wait after gate opens)
- internal delay: 7 ns
- Gate width: 30ns-10µs
- Digitizing time 106 µs (+ Gate width = time to LAM)
- Important functions F for communication:
    - F(0): read
    - F(8): Test LAM
    - F(9): clear module and LAM
    - F(26): Enable LAM (Look-At-Me)
    - C,I: Clear, Initialize module

5.2.5.3 CAEN C414 8CH TDC

- Available jumper settings: 100ns,200ns,500ns equivalent 12bit (FFF)
- Important functions F for communication:
    - F(0): read
    - F(8): Test LAM
    - F(9): clear module and LAM
    - F(26): Enable LAM (Look-At-Me)
    - C,I: Clear, Initialize module

5.2.5.4 CAEN C257 SCALER

- Important functions F for communication:
    - F(0): read
    - F(9),C,Z: reset
- One has to be careful, because when read out, the order of the channels is shifted. Connected: 1,2,3,4 readout: 4,1,2,3
- Further the very first readout cycle on the last channel (e.g. 4) gives a random output.

5.2.6 NIM System

5.2.6.1 Phillips Scientific 804, Quad Rotary Step Attenuator

5.2.6.2 Signal splitter 20/80

Due to intolerable reflections in the LEMO Y-connectors, this self-made slot was used to split the signal. It is not really a NIM module, since it is just a front panel with a Y-connection of resistances (0Ω,200Ω,and 12Ω) and mounting screws, but it was essential for the measurements. It is important to consider the reduction of the signal for choosing the thresholds. It is crucial that the trigger uses the stronger signal, otherwise it would not work.

5.2.6.3 CAEN N405 Fold Logic

Delay 14±2ns

5.2.6.4 Canberra 2017A Dual Counter Timer

5.2.6.5 LeCroy 821 Quad Discriminator

Delay 9.5 ns

Threshold / 10 = [mV]

5.2.6.6 Phillips Scientific 706, 16Ch Discriminator

Delay 9 ns

5.2.6.7 PSI LD100 Logic Delay

5.2.6.8 PSI D105 Delay

5.2.6.9 CAEN N93B Dual Timer

5.2.6.10 BNC Pulse Generator PB-1

5.2.6.11 Level converter

5.2.7 Cooling and temperature measurement equipment

- Rittal Sk3318.600 (water cooling)
- Lake Shore 120 Current Source (for Pt-100)
- Supercool Peltier element (30x30x6.2mm; 2 rows, no datasheet available, tested to 1.6A max.)
- Wavelength Electronics MPT-5000 (Peltier element controller)
  The device is stabilizing the temperature while comparing a set-point to the measured voltage ofa thermistor. It is able to heat and cool that is why the negative voltage should not be connected to ground.(Otherwise the regular operation is not possible and this can damage other measurement devices.) One can choose to supply it between 5V to 15V (which limits the maximum Peltier thermal power output). The set point can be adjusted locally on a potentiometer (between 0-5V) and on an analogue connector (2V/V). The set point and actual temperature (in V) can be monitored.

5.2.8 Power Supplies

- Delta Elektronika Power Supply ES030-10
- Keithley 6517 Electrometer/high resistance system

5.2.9 Various measurement devices (standalone)

- Tektronix TDS 7104 Oscilloscope
- Picotest Universal Counter U6200A
- National Instruments DAQ, NI USB_6009
- Keithley 199 DHM
- Fluke 87 V

5.2.10 Other Devices (standalone)

- HP 8082A Pulse Generator
- Stanford Research Systems Digital Delay Generator DG535 Digital delay / pulse generator (4 Ch.)

5.2.11 Radioactive source

- In Order to get a signal for calibration respectively measuring, I used a solid sealed Canberra[7] Na-22 source. The sealing is a 25mm by 3mm plastic disk.
- 10 µCi T½ = 2.6a
- Gamma: 511 keV 1274.5 keV
- e+ source

To reach maximum potential, the source needs to be directed with the non-foiled side to the detector.

7 www.canberra.com

TABLE OF FIGURES

Glossary

LAM

Look-At-Me

PPD

Pixelized Photo Multiplier; See SiPM, respectively 2.2, p. 11

SDD

Silicon Drift Detector; *See* Bibliography

SIDDHARTA

Silicon Drift Detector for Hadronic Atom Research by Timing Application; *See 1.1* What is SIDDHARTA?

SiPM

Silicon Photo Multiplier; *See 2.2*

Bibliography

[1] SIDDHARTA Collaboration, M. Bazzi, et.al, Phys. Lett. B 704 (2011) 113

[2] SIDDHARTA Collaboration, M. Bazzi, et.al, Phys. Lett. B 697 (2011) 199

[3] SIDDHARTA Collaboration, M. Bazzi, et.al, Phys. Lett. B 714 (2012) 40

[4] SIDDHARTA-2 Collaboration, SIDDHARTA-2 Proposal (2010), https://www.lnf.infn.it/committee/private/documenti/SIDDHARTA2-proposal_FINAL.pdf

[5] SIDDHARTA-2 Collaboration, SIDDHARTA-2 the kaonic deuterium case (2011) https://www.lnf.infn.it/committee/private/documenti/SIDDHARTA-2_Kd_April-2011.pdf

[6] M. Doering, U-G.Missner, Phys. Lett. B 704 (2011) 663

[7] C. Fiorini, et al., Nucl. Instr. Meth A 568 (2006) 322

[8] M. Bazziet. al., Nucl. Instr. Meth A 628 (2011) 264

[9] T. Ishiwatari et. al., Proposal of Measurement of kaonic deuterium X-rays, FWF P24756-N20

[10] G. S. M. Ahmed et. al., Nucl. Instr. Meth. A 628 (2011) 393

[11] J. Haba, Nucl. Intr. Meth A 595 (2008) 154

[12] Hamamatsu Corporation,

http://sales.hamamatsu.com/en/products/solid-state-division/si-photodiode-series/mppc.php